NASA TN D-322



# TECHNICAL NOTE

## D-322

INVESTIGATION OF THE ERRORS OF AN INERTIAL GUIDANCE SYSTEM DURING SATELLITE RE-ENTRY

By John S. White

Ames Research Center
Moffett Field, Calif.

NATIONAL AERONAUTICS AND SPACE ADMINISTRATION
WASHINGTON
August 1960

NATIONAL AERONAUTICS AND SPACE ADMINISTRATION

TECHNICAL NOTE D-322

# INVESTIGATION OF THE ERRORS OF AN INERTIAL GUIDANCE SYSTEM DURING SATELLITE RE-ENTRY

By John S. White

## SUMMARY

During the re-entry phase of a manned satellite, some equipment for continuous on-board indication of position will be required. Since radio and radar may be useless during part of the re-entry, inertial guidance equipment may be required. Such equipment, however, has an inherent instability in the computation of altitude.

The present study of an inertial guidance system shows that for reasonable values of initial-condition errors and equipment biases, the resultant position indication errors will not become excessive unless the re-entry maneuver time is greater than 45 minutes to an hour. Further, the position indication error caused by accelerometer uncertainties can be reduced by switching off the accelerometers until their output becomes significantly greater than their uncertainty.

## INTRODUCTION

For a manned satellite vehicle re-entering the earth's atmosphere to land at a particular spot on the earth, the pilot must continuously know his spatial position, velocity, and attitude. Before re-entry, this information can be obtained either from on-board sources or, in the case of position and velocity, from ground-based radars with telemetering to the vehicle.

However, during the actual re-entry, the vehicle will be surrounded by a layer of hot ionized gas and, at altitudes less than about 350,000 feet, may not be able to communicate with the ground via radio or radar. Radio contact with the ground probably would be re-established by the time the vehicle reached an altitude of about 150,000 feet. Thus, for the interval between 350,000 and 100,000 feet, a self-contained on-board source of position information - an inertial navigation system - probably will be required. A system consisting of a gyro reference platform to maintain an orientation in space, an accelerometer package mounted with the gyros to measure the vehicle accelerations, and a computer to determine position, velocity, and attitude from the outputs of the accelerometers and gyros would be capable of measuring position and velocity

fairly accurately over long periods of time if it had a suitable means of determining altitude. Present radar or barometer systems used in aircraft for sensing altitude would not be suitable.

Under the above conditions, the inertial guidance system of a re-entry vehicle would have to compute its own altitude. The equations for doing so have, at suborbital speeds, an unstable solution, that is, one in which any incorrect initial condition or error in acceleration measurement will cause an error in altitude indication which will grow exponentially with time (see appendix). The time constant of the solution is considerably less than the satellite re-entry time. For this reason it seems imperative to make an investigation of the errors that may occur in an inertial guidance system during re-entry. In particular, can the error caused by incorrect measurement of the acceleration be reduced, perhaps by switching out the accelerometers for a period of time during the re-entry? The present report presents the results of such an investigation.



## LIST OF SYMBOLS

| | |
|---|---|
| $A$ | reference area for aerodynamic force coefficients |
| $C_D$ | drag coefficient |
| $\frac{C_D A}{m}$ | vehicle constant relating drag to airspeed and air density |
| $D$ | aerodynamic drag per unit mass, $ft/sec^2$ |
| $F$ | force per unit mass, $ft/sec^2$ |
| $f$ | nongravitational force per unit mass, $ft/sec^2$ |
| $g$ | gravitational attraction of earth per unit mass, $ft/sec^2$ |
| $g_r$ | gravitational attraction of earth per unit mass at sea level, 32.1279 $ft/sec^2$ |
| $h$ | altitude above sea level, ft |
| $L$ | aerodynamic lift per unit mass, $ft/sec^2$ |
| $m$ | mass of vehicle, slugs |
| $R$ | distance from satellite to center of earth, ft |
| $R_r$ | radius of earth, $0.209102 \times 10^8$ ft |

| | |
|---|---|
| $T$ | thrust per unit mass from retrorocket, $ft/sec^2$ |
| $t$ | time, sec |
| $U$ | uncertainty of accelerometer reading, $ft/sec^2$ |
| $V_A$ | velocity of satellite relative to the air mass, ft/sec |
| $\alpha,\beta,\gamma$ | axes of satellite coordinate system |
| $X,Y,Z$ | axes of indicated satellite coordinate system |
| $X_p,Y_p,Z_p$ | axes of platform coordinate system |
| $X_{po},Y_{po},Z_{po}$ | axes of platform coordinate system at $t = 0$ |
| $\bar{\alpha},\bar{\beta},\bar{\gamma}$ | unit vectors along satellite coordinates |
| $\Delta V$ | velocity increment at initial altitude |
| $\gamma_A$ | flight-path angle - angle from true horizontal to $\bar{V}_A$, positive up, radians |
| $\rho$ | air density, slugs/cu ft |
| $\varphi$ | supplement of angle between $X_p$ and $\bar{T}$, radians |
| $\theta$ | range angle, measured at the center of the earth between a reference line and the vertical, radians |
| $\tau_1,\tau_2,\tau_3,$ $\tau_4,\tau_{4X},\tau_{4Z}$ | specific times during a re-entry, sec |
| $\omega$ | angular velocity with respect to inertial space, radians/sec |
| $\omega_d$ | gyro drift rate, radians/sec |
| $\omega_e$ | earth angular velocity, $0.7292 \times 10^{-4}$ radian/sec |

Superscripts

| | |
|---|---|
| $\bar{}$ | vector |
| $\dot{}$ | time derivative |

Subscripts

| | |
|---|---|
| i | indicated quantity |
| 0 | value at $t = 0$ |
| $\epsilon$ | error between indicated and true |
| $\alpha, \gamma$ | components of vector along $\alpha$ and $\gamma$ axes |
| x,z | components of vector along X and Z axes |
| m | measured quantity |



## GENERAL CONSIDERATIONS

The approach used was to solve both the equations of actual motion of the satellite in response to the actual forces and the equations of indicated motion (used by the inertial guidance equipment) in response to measured forces. The latter equations have in them the initial-condition errors and equipment biases that might reasonably be expected to occur. The two sets of results were then compared to ascertain the position and velocity errors of the inertial guidance equipment.

These errors were studied as functions of initial-condition errors, equipment biases, orbiting altitude, vehicle lift-to-drag ratio, and re-entry maneuver. The effect of having the accelerometers switched out for various periods during re-entry was also ascertained. To simplify the equations, it was assumed that the vehicle moves easterly in the equatorial plane and that the earth is spherical. These simplifying assumptions are justified since we are trying to isolate the errors caused by the inertial navigation system. Similarly, small discrepancies between the actual and assumed atmospheric density profiles will not affect the errors caused by the inertial navigation equipment.

A set of basic conditions was chosen for use during this study and then various parameters were changed to study their effects on the errors. The standard vehicle was assumed to have an L/D of 0.5 with a $C_DA/m$ of 0.533. The basic initial altitude was 677,000 feet and the basic velocity increment, $\Delta V$, selected was 250 feet per second. This and all other values of $\Delta V$ were developed by applying a 1g thrust at an angle of $45^\circ$ down and to the rear of the flight path, for that length of time which was necessary to develop the desired $\Delta V$.

For these conditions, the position errors resulting from accelerometer biases and gyro drift, both singly and collectively, were determined by computation on a digital computer. The effects of initial-condition

errors were also determined, both singly and collectively, and finally the effect of switching out the accelerometers for various periods of time immediately following retrothrust was determined.

The effects of accelerometer biases and gyro drifts were then determined for two other altitudes, two other vehicles (a zero-lift vehicle with $C_DA/m$ of 1.0, and a glider with $C_DA/m$ of 0.158 and L/D of 1.0), and two other values of $\Delta V$ (at the same angle). For all of these digital-computer runs the effects of switching out the accelerometers were determined.

As used in this report, uncertainty of a quantity implies an imperfect knowledge of that quantity. Thus, for example, the accelerometer output is equal to the actual value of the acceleration plus the accelerometer uncertainty. An uncertainty has a random component plus a quasi-steady component. The latter component is referred to in this report as bias.

A 3 9 9

## Coordinate Systems

Two basic coordinate systems are used in this report. Both are right-handed, orthogonal, and centered in the satellite, with one axis forward and one axis down. One is the normal aircraft system (here called the satellite coordinate system) with coordinates $\alpha$, $\beta$, and $\gamma$, in which the $\gamma$ axis is along the true vertical (toward the center of the assumed spherical earth) and the $\alpha$ axis is forward. The other coordinate system, called the indicated satellite coordinate system, is derived by the on-board computer, and is used to determine the indicated position of the vehicle. It has coordinates X, Y, and Z, with the Z axis along the indicated vertical. Since the problem is solved in a single plane, the Y and $\beta$ axes coincide.

Two additional coordinate systems are used as references. One is the platform coordinate system, with coordinates $X_p$, $Y_p$, and $Z_p$, such that $Y_p$ coincides with Y and $\beta$. The platform is designed to be inertially fixed, and the on-board computer assumes that it is. However, there will actually be some rotation of the platform caused by gyro drift. The other reference coordinate system represents the location of the platform coordinate system at time zero and is inertially fixed. Its coordinates are $X_{po}$, $Y_{po}$, and $Z_{po}$. Again, $Y_{po}$ coincides with Y, $\beta$, and $Y_p$. The angular motion of the platform system with respect to the inertially fixed system is about the $Y_p$ axis and represents gyro drift. The $Z_{po}$ axis is chosen along the initial true vertical.

Figure 1 shows the four coordinate systems and the various vectors used in this report. The vectors $\beta$, Y, $Y_p$, $Y_{po}$, and $\omega$ are perpendicular to, and coming out of, the page.

## DERIVATION OF EQUATIONS

### Equations of Motion of the Satellite

The motion of the center of mass of the satellite can be expressed in an inertially fixed coordinate system as:

$$\ddot{\overline{R}} = \overline{F} \tag{1}$$

where $\overline{F}$ is the total force per unit mass exerted on the body. This force can be divided into two parts: $\overline{g}$, the gravitational attraction of the earth, and $\overline{f}$ which consists of the lift, $\overline{L}$, drag, $\overline{D}$, and the thrust, $\overline{T}$. All forces other than those mentioned above have been neglected.



Equation (1) can be written in an earth-centered coordinate system, rotating at an angular velocity with respect to inertial space of $\omega$ by means of the rule of Coriolis, as follows (ref. 1, p. 342):

$$\ddot{\overline{R}} + \overline{\omega} \times (\overline{\omega} \times \overline{R}) + 2\overline{\omega} \times \dot{\overline{R}} + \dot{\overline{\omega}} \times \overline{R} = \overline{F} \tag{2}$$

where

$$\overline{F} = \overline{g} + \overline{f} = \overline{g} + \overline{L} + \overline{D} + \overline{T}$$

This equation is also valid when expressed in terms of a satellite coordinate system, where $\gamma$ is toward the earth center, and $\omega$ is the orbital angular velocity.

Expressing the quantities used in equation (2) in this satellite coordinate system gives:

$$\left.\begin{aligned} &\overline{R} = -(R_r + h)\overline{\gamma} \qquad \dot{\overline{R}} = -\dot{h}\overline{\gamma} \qquad \ddot{\overline{R}} = -\ddot{h}\overline{\gamma} \\ &\overline{\omega} = -\dot{\theta}\overline{\beta} \qquad\qquad \dot{\overline{\omega}} = -\ddot{\theta}\overline{\beta} \qquad \overline{g} = \frac{g_r R_r^{\,2}}{(R_r + h)^2}\,\overline{\gamma} \end{aligned}\right\} \tag{3}$$

It should be noted that the angle $\theta$ is defined so that it will increase positively as the satellite moves around the earth, and does <u>not</u> follow the usual right-hand rule for angles and angular velocities in the satellite coordinate system. Also, $\theta$ is measured with respect to an inertially fixed reference, and not with respect to the rotating earth.

Substituting equation (3) into equation (2), we get

$$-\ddot{h}\bar{\gamma} + (R_r + h)\dot{\theta}^2\bar{\gamma} + 2\dot{h}\dot{\theta}\bar{\alpha} + (R_r + h)\ddot{\theta}\bar{\alpha} = \frac{g_r R_r^2}{(R_r + h)^2}\bar{\gamma} + f_\alpha\bar{\alpha} + f_\gamma\bar{\gamma} \tag{4}$$

where $f_\alpha$ and $f_\gamma$ are the components of $\bar{f}$ along $\alpha$ and $\gamma$, respectively, and $f_\beta = 0$, since we are assuming a two-dimensional problem.

These equations can now be separated into their $\alpha$ and $\gamma$ components, giving



$$\left.\begin{aligned} \ddot{h} - (R_r + h)\dot{\theta}^2 &= -\frac{g_r R_r^2}{(R_r + h)^2} - f_\gamma \\ (R_r + h)\ddot{\theta} + 2\dot{h}\dot{\theta} &= f_\alpha \end{aligned}\right\} \tag{5}$$

which describe the actual motion of the center of mass of the satellite in response to the forces $g$, $f_\alpha$, and $f_\gamma$.

The force $\bar{f}$ can be determined by summing vectorially the lift, drag, and thrust of the vehicle as shown in equation (2).

The equations for the magnitude of $\bar{D}$ and $\bar{L}$ are

$$\left.\begin{aligned} D &= (1/2)\rho V_A^2 (C_D A/m) \\ L &= (L/D)D \end{aligned}\right\} \tag{6}$$

These quantities are directed antiparallel and perpendicular, respectively, to the vector representing the velocity of the satellite with respect to the air mass. The quantity $C_D A/m$ is a constant of the vehicle, and it is assumed that the vehicle angle of attack is controlled so that the quantity $L/D$ is also constant. The air density, $\rho$, was taken from the standard ARDC atmosphere (ref. 2) for altitudes below 332,000 feet, and from the Sputnik atmosphere for higher altitudes (ref. 3).

The retrothrust, T, is used only during the initial portions of the re-entry to change the vehicle motion from orbital to re-entry. It is applied along a body axis, which is assumed to be maintained, during the thrust period, in a specified orientation, $\varphi$, with respect to the inertial platform. Following the thrust period, the body is controlled to maintain constant $L/D$.

Resolving $\bar{f}$ into $f_\alpha$ and $f_\gamma$ gives:

$$\left.\begin{aligned} f_\alpha &= -L \sin \gamma_A - D \cos \gamma_A - T \cos(\theta + \varphi - \omega_d t) \\ f_\gamma &= -L \cos \gamma_A + D \sin \gamma_A + T \sin(\theta + \varphi - \omega_d t) \end{aligned}\right\} \quad (7)$$

Then substituting equation (6) into equation (7), we get

$$\left.\begin{aligned} f_\alpha &= -\frac{1}{2} \rho V_A^2 \frac{C_D A}{m} \left(\cos \gamma_A + \frac{L}{D} \sin \gamma_A\right) - T \cos(\theta + \varphi - \omega_d t) \\ f_\gamma &= \frac{1}{2} \rho V_A^2 \frac{C_D A}{m} \left(\sin \gamma_A - \frac{L}{D} \cos \gamma_A\right) + T \sin(\theta + \varphi - \omega_d t) \end{aligned}\right\} \quad (8)$$

A 3 9 9

The following sketch shows the derivation of $V_A$ and $\gamma_A$ from satellite and earth velocities.[1]

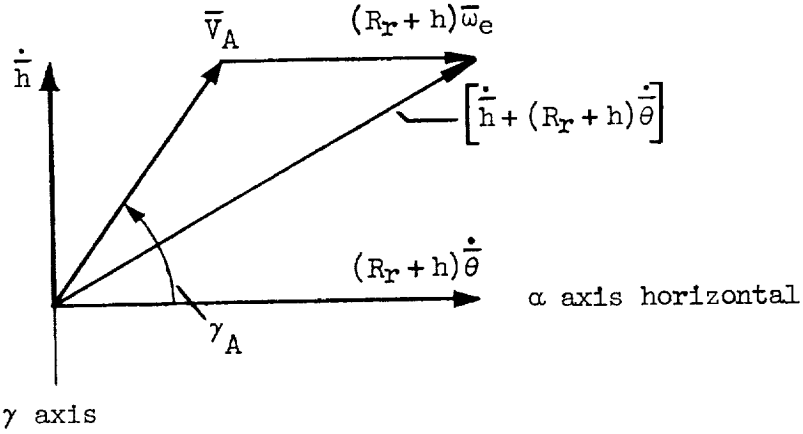


From the sketch, we get the following equations:

$$\left.\begin{aligned} V_A^2 &= \dot{h}^2 + (R_r + h)^2(\dot{\theta} - \omega_e)^2 \\ \gamma_A &= \tan^{-1} \frac{\dot{h}}{(R_r + h)(\dot{\theta} - \omega_e)} \end{aligned}\right\} \quad (9)$$

---

[1]The constant $(R_r + h)\omega_e$ is the velocity of the air mass with respect to inertial space for an atmosphere which is assumed to be rigidly attached to the earth and to move with it. Since this velocity lies in the equatorial plane, its use assumes that $\bar{V}_A$ and $\bar{V}$ are also in this plane and that the vehicle is thus in an equatorial orbit moving in an easterly direction.

Equations (5), (8), and (9), and the atmospheric table describe completely (within the limits of the assumptions) the motion of the satellite.

## Inertial Navigation Equations

Since equations (5) describe the motion of the satellite in response to gravity and the force $\bar{f}$, these equations can also be used by the on-board computer to determine satellite position in response to the measured forces and computed gravity. The equations then become, expressed in computer quantities,



$$\left.\begin{aligned} \ddot{h}_i - (R_r + h_i)\dot{\theta}_i^2 &= -f_{zm} - \frac{g_r R_r^2}{(R_r + h_i)^2} \\ \ddot{\theta}_i(R_r + h_i) + 2\dot{h}_i\dot{\theta}_i &= f_{xm} \end{aligned}\right\} \qquad (10)$$

Here $f_{xm}$ and $f_{zm}$ are components of the measured forces, in the indicated horizontal and vertical directions, respectively.[2] The accelerations are actually measured in platform coordinates. The accelerometer outputs can thus be obtained by resolving the true forces, $f_\alpha$ and $f_\gamma$, into platform X and Z components through the angle $(-\theta + \omega_d t)$ (see fig. 1) and then adding in the uncertainties of measurement $U_{xp}$ and $U_{zp}$. These accelerometer outputs must then be resolved through the angle $\theta_i$ to obtain $f_{xm}$ and $f_{zm}$. Both of these resolutions were done simultaneously, giving the following equations:

$$\left.\begin{aligned} f_{xm} &= f_\alpha \cos(-\theta + \omega_d t + \theta_i) + f_\gamma \sin(-\theta + \omega_d t + \theta_i) \\ &\quad + U_{xp} \cos\theta_i + U_{zp} \sin\theta_i \\ f_{zm} &= f_\gamma \cos(-\theta + \omega_d t + \theta_i) - f_\alpha \sin(-\theta + \omega_d t + \theta_i) \\ &\quad + U_{zp} \cos\theta_i - U_{xp} \sin\theta_i \end{aligned}\right\} \qquad (11)$$

---

[2] The quantities $f_{xm}$ and $f_{zm}$ are the components of the accelerometer output (force per unit mass) in indicated horizontal and vertical directions; $g_r R_r^2/(R_r + h_i)^2$ is the computed gravity term which must be added to the accelerometer output to determine the actual linear acceleration.

## Error Equations

We now have equations describing the actual motion of the satellite in response to the actual forces (eq. (5)), and the motion as indicated by the inertial navigation equipment, in response to the measured forces (eq. (10)). The errors of the indicated quantities can be defined as

$$\left.\begin{aligned} h_\epsilon &= h_i - h \\ \dot{h}_\epsilon &= \dot{h}_i - \dot{h} \\ \theta_\epsilon &= \theta_i - \theta \\ \dot{\theta}_\epsilon &= \dot{\theta}_i - \dot{\theta} \end{aligned}\right\} \qquad (12)$$

A 3999

## Initial Conditions

Equations which describe the motions of any orbital vehicle (within the limits of our assumptions) have been derived, and now the initial conditions must be defined. For this problem, we assume that the vehicle has been traveling in a circular orbit at the specified initial altitude $h_o$ (and therefore $\dot{h}_o = \ddot{h}_o = 0$) and that the aerodynamic forces $f_\alpha$ and $f_\gamma$ while in orbit are also zero. Using the first of equations (5), we get

$$\dot{\theta}_o = \left[\frac{g_r R_r^{\,2}}{(R_r + h_o)^3}\right]^{1/2} \qquad (13)$$

The value of $\theta_o$ was arbitrarily chosen to be zero.

The initial conditions for the indicated equations (10) are ideally identical to those used for the actual motion of the vehicle. However, in practice there will be errors in the indication of position and velocity just prior to retrothrust which will alter these initial conditions as follows:

$$\left.\begin{aligned} h_{io} &= h_o + h_{\epsilon o} \\ \dot{h}_{io} &= \dot{h}_o + \dot{h}_{\epsilon o} \\ \theta_{io} &= \theta_{\epsilon o} \\ \dot{\theta}_{io} &= \dot{\theta}_o + \dot{\theta}_{\epsilon o} \end{aligned}\right\} \qquad (14)$$

The effect on the initial conditions of drift of the gyro reference coordinate system prior to retrothrust must be considered also, as follows: $\theta$ is measured from the inertial space reference, $Z_{po}$, to the local vertical, $\gamma$; $\theta_i$ is measured from the platform reference, $Z_p$, to the indicated vertical, Z. In the presence of gyro drift prior to retrothrust $Z_p$ and $Z_{po}$ will not be parallel at time zero, and thus, although $\theta_i$ and $\theta$ may be equal, the indicated and true verticals will not be parallel. Since, in the solution of the problem, $Z_{po}$ is assumed along $Z_p$ at time zero, we can allow for these nonparallel initial verticals by letting $\theta_{\epsilon o}$ be nonzero and equal to the gyro drift angle to be considered.

Thus, $\theta_{\epsilon o}$ can be used to represent two errors: One is the initial error in position indication from either the airborne equipment or ground measurements of satellite position. The other is the error in reference orientation due to platform drift prior to retrothrust. Both of these sources of error are considered.



## METHOD OF SOLUTION

### Computation Equipment Used

Equations (5), (8), (9), (10), (11), and (12) must now be solved simultaneously to determine the various errors where equations (13) and (14) specify the initial conditions. This cannot be done analytically. Although the equations could be set up on an analog simulator, the answers would be highly inaccurate, since in several places it is necessary to subtract nearly equal numbers. The use of a digital computer, in particular the IBM 704, was indicated as the means of solving these equations. Accordingly, these simultaneous ordinary differential equations were programmed for the IBM 704, using single precision floating decimal point arithmetic. In the computations, a subroutine applying the Adams-Moulton and Runge-Kutta integration techniques was used. Double precision arithmetic is found within this subroutine to control round-off error. The variable step-size mode of integration was used; therefore, the program can determine each interval size sufficiently small that the truncation error per integration step is always less than some specified value. While the program guarantees that the local error is less than this value, the cumulative error usually exceeds it. For this problem, it was desired to use all of the accuracy available from the IBM 704. Thus, the truncation error per step was specified as less than one part in $10^7$, so that all the digits of each number were retained.

## Form of Solution

The inertial navigation equipment aboard would be used during most of the phases of operation of the satellite vehicle. During lift-off and boost, the equipment would continuously compute vehicle position, using equation (10). At cutoff, the on-board computer would have determined the vehicle velocity and position, and would use these values to continuously compute its position in orbit. This could be done using equation (10), with $f_{xm} = f_{zm} = 0$. However, a more accurate method would be to determine the six elements of the orbit and their variation with time, and from these to compute the vehicle position. While the vehicle is orbiting, this position information would probably be corrected by ground measurements of vehicle position, and gyro drift effects might be eliminated by stellar monitoring.



For this study, we have assumed that the on-board computer will use equation (10) to determine position and velocity during re-entry. At time $t = 0$, we assume that the computer is solving this equation and, since the retrothrust is to begin momentarily, the accelerometer outputs $f_{xm}$ and $f_{zm}$ are being used in this equation.

At time $\tau_1$, arbitrarily chosen to be at 10 seconds, the retrothrust rockets are fired. The rocket acceleration is preselected as T, equal to 1 g, and a specified value of nominal change in velocity, $\Delta V$, and direction of thrust, $\varphi$, is chosen. Then $\tau_2$ can be computed as follows:

$$\tau_2 - \tau_1 = \frac{\Delta V}{T}$$

The rocket is then turned off at time $\tau_2$.

For those cases where it was desired to switch out the accelerometer input to the computer subsequent to retrothrust firing, a time $\tau_3$, 10 seconds later than $\tau_2$, was selected as the accelerometer switch-out time; that is, subsequent to $\tau_3$, the acceleration input to the computer was assumed to be zero. The final switch-in of the accelerometers then occurred at $\tau_4$. In some cases, this was a preselected time following $\tau_3$. In other cases, the outputs of the accelerometers were used as an indication of when they should be switched in. That is, the value of $f_{xm}$ and $f_{zm}$, after resolution into indicated coordinates, was compared with the assumed uncertainty of measurement. When $f_{xm}$ or $f_{zm}$ became significantly greater than this uncertainty, the respective accelerometer output was applied to the indicated position equations (10). Since $f_{xm}$ and $f_{zm}$ might become significant at different times, the X and Z accelerometers were switched in at $\tau_{4X}$ and $\tau_{4Z}$, respectively. These times were not necessarily simultaneous, and either one could occur first.

For all cases, the indicated position errors are computed down to an altitude of 100,000 feet. It is assumed that at this altitude the inertial navigation equipment can obtain altitude information from barometric pressure and, since communication with the ground has been re-established, that position, altitude, and velocity can be checked against a radar altimeter and the telemetered ground information, so that further indication errors could be corrected.

## Error Magnitudes

Before computing the indication errors resulting from erroneous initial conditions and equipment biases and uncertainties, it is necessary to know the probable magnitudes of these initial condition and equipment errors.

First, consider initial condition errors. Assume that radar or the on-board inertial guidance equipment will compute the burnout position to within approximately 200 feet and the corresponding velocity to within 1 foot per second in magnitude and within $0.003^{\circ}$ in orientation. Converting these quantities into the form in which they are used here, we have at burnout an altitude error of ±200 feet, a range error of $\pm 10^{-5}$ radian, an altitude rate error of ±1 foot per second, and a range rate error of $\pm 5 \times 10^{-8}$ radian per second.

If the equations previously derived are used to determine the vehicle position while orbiting, the indication errors will increase as a function of the number of orbits. In particular, after two orbits, the range error $\theta_{\epsilon}$ will increase to $\pm 14 \times 10^{-4}$ radian and the altitude error to around 400 feet while $\dot{h}_{\epsilon}$ and $\dot{\theta}_{\epsilon}$ will remain about the same size. This assumes that the average effect of drag on the satellite is considered in computing the indicated position. If this drag is neglected, these errors will build up very much larger. However, with orbital corrections from the ground, plus a position fix just prior to firing of the retrorocket, it is assumed that the values of the initial condition errors at $t = 0$ might be as follows:

$h_{\epsilon O} = 500$ feet $\qquad\qquad \theta_{\epsilon O} = 10^{-4}$ radian

$\dot{h}_{\epsilon O} = 1$ foot per second $\qquad\qquad \dot{\theta}_{\epsilon O} = 5 \times 10^{-8}$ radian per second

These values were chosen as nominal values for the initial condition errors although other values were also studied.

The effect of equipment uncertainties was also considered. In general, the imperfections of gyros show up as gyro drift rate. Relatively poor gyros were assumed for this study, and a value for $\omega_d$ of $2 \times 10^{-7}$ radian per second, or about $0.04^{\circ}$ per hour, was chosen as a nominal drift rate although, again, other values were tried. Imperfections in an accelerometer show up as an uncertainty in the output. This

uncertainty consists of two components, a quasi-steady error, and a random error. During any one entry, the system errors due to the random component will more or less cancel and can be ignored. The quasi-steady error may vary slowly throughout an entry, and will be random over an ensemble of entries. Therefore, this term will create a system error which must be considered. In order to avoid the necessity for statistical measurements of the resultant errors, a specific bias value, constant throughout a run, was assumed which would give the largest errors, that is, the worst possible case. The results can then be interpreted as defining an envelope of error within which it can be expected that all errors will be found. The bias value principally used was $10^{-4}$ g, which corresponds to a relatively poor accelerometer.



It should be noted that because the accelerometer axes are nominally fixed in spatial direction, the direction of the bias is also fixed in space. However, since the indicated coordinate system is rotating around the earth, the biases must be resolved through the indicated range angle before being used in the on-board computer, as shown in equation (11). As long as the range angle remains small, the concept of envelope of error from accelerometer bias is applicable. However, when the range angle becomes greater than $90^{\circ}$, some of the effects of accelerometer bias change sign, so that this envelope concept is no longer applicable.

## RESULTS AND DISCUSSION

Figure 2 shows the flight path profile for each of the various conditions. It can be seen in figure 2(a) that different vehicles, starting from the same altitude with the same value of $\Delta V$, follow the same path to an altitude of about 300,000 feet before diverging. All the trajectories are smooth curves, essentially Keplerian, until this altitude is reached. Thus, 300,000 feet is the altitude at which the air density becomes great enough to noticeably alter the flight path. At altitudes higher than this the flight path is essentially Keplerian, with, however, some very small deviations due to the residual air density.

All these runs were computed down to an altitude of 100,000 feet except the Keplerian orbits, and the end of each run is indicated by an asterisk. On subsequent figures, an asterisk is placed on each curve at a time which corresponds to the vehicle reaching 100,000 feet.

Figure 2(c) shows the range profile for these same conditions. For all vehicles and all entry conditions the Keplerian range profiles are essentially identical and are drawn as one curve. The actual range profile deviates slightly from this Keplerian value at altitudes below 300,000 feet.

Figure 2(d) is a curve of acceleration versus altitude. It shows that above 300,000 feet the acceleration level for a given vehicle is independent of both the initial altitude and the initial re-entry maneuver.

For example, for the standard vehicle, the $f_\alpha$ curve is independent of $\Delta V$ and $h_o$, as is the $f_\gamma$ curve. Different vehicles, however, have different acceleration levels. This would indicate that, for a given vehicle, it would be satisfactory to switch the accelerometers in as a function of Keplerian indicated altitude, rather than as a function of accelerometer output.

Re-entry runs were made under many different conditions, with different error producing sources of different magnitudes, singly and collectively. Study of the resultant errors of these systems showed that altitude error seemed to be the best criterion for judging whether or not a particular error-producing source caused excessive errors. The actual magnitude of the altitude error varied from 0 to ±20,000 feet.



The effect on the altitude error of various initial-condition errors applied individually is shown in figure 3(a) for the standard vehicle ($C_DA/m = 0.533$, $L/D = 0.5$) starting from $h_o = 677{,}000$ feet with $\Delta V = 250$ feet per second. It can be seen that initial altitude errors and range rate errors cause the largest altitude error. Plotted on the same figure is a curve for an initial range error of $2.16 \times 10^{-3}$ radian. This would correspond to a gyro drift rate of $2 \times 10^{-7}$ radian per second ($0.04^\circ$/hr) for a period of approximately 3 hours, or two orbits. The resultant altitude error at 100,000 feet is large, indicating that gyro drift rates of this magnitude probably can not be tolerated while orbiting. They must either be corrected by stellar monitoring or by the use of better gyros.

The effects of various other magnitudes of initial-condition errors were studied both singly and collectively. In spite of the nonlinear equations, the results indicated that the resultant altitude error was linearly proportional to the magnitude of the initial-condition error, and that the superposition theorem could be used to determine the effects of initial-condition errors collectively; that is, the result for initial-condition errors applied simultaneously is equal to the sum of the results for each of these errors applied individually.

These altitude errors are principally a function of time so that if a re-entry is of longer duration, the error will be worse. Figure 3(b) shows this effect for three different conditions. It should be noted that for both conditions of the standard vehicle the error at 300,000 feet is around 1/3 of the total error at 100,000 feet, and that the error build-up occurs most rapidly during the last few hundred seconds. Thus the altitude error at the end of the run caused by incorrect initial conditions can be considerably reduced if the run can be made somewhat shorter, that is, if altitude can be determined from external means somewhat sooner.

The accelerometer biases and gyro drifts were studied separately and collectively, and in combination with initial-condition errors. In every case, the error due to a combination of error-producing sources was equal to the sum of the errors from the error sources individually.

In addition, the error was directly proportional to the magnitude of the error source. Thus data which have been taken for one particular magnitude for each error-producing source may be scaled according to the magnitude of the expected actual error source, and then the results for several error sources may be combined to give an estimated value of total error.

Figure 4 shows the altitude error versus time for different re-entries during which there was gyro drift. The reference time used in plotting this figure was that time at which the satellite passed through 300,000 feet altitude, which is where the air density effects first become noticeable. For those cases where $\omega_d = 2\times10^{-7}$, there is no appreciable altitude error due to gyro drift until about 300 seconds after $t_{ref}$. This is to be expected, since gyro drift rotates the platform containing the accelerometers, and this has no affect until the accelerometers have an appreciable output (below 300,000 ft). The build-up of the altitude error due to gyro drift is a function of time of drift and the magnitude of the acceleration. For the 900,000-foot-altitude case, the re-entry time was considerably longer than for the 677,000-foot case, which would imply greater errors. However, the acceleration level was, in general, considerably lower, implying smaller errors. These two effects combined to give a net reduction of error at any particular time following $t_{ref}$ but an increased error at the end of the run.

The curve of figure 4 for the larger value of $\omega_d$ shows that the altitude error is proportional to the magnitude of the gyro drift.

Figure 5 shows the altitude error caused by accelerometer biases. It can be seen that the altitude error caused by $U_{xp}$ is smaller than that caused by $U_{zp}$ during the early portions of a run, but then builds up considerably larger in the later portions of the run.

The effect of $U_{zp}$ on altitude error shows a reversal in sign. This is caused by the interaction of the bias, $U_{zp}$, as it is resolved, the centrifugal acceleration term in the vertical equation (see eq. (11)), and the altitude error itself. For the longer runs, the bias error, as resolved through the range angle, and the resultant centrifugal acceleration error combine to cause the error reversal. For the shorter runs, these terms become insignificant much sooner, and the existing altitude error prevents the sign reversal.

The same divergence is noticeable on the runs with $U_{xp}$ accelerometer bias. However, it is not so pronounced since there is no sign reversal until the range angle becomes $180^{\circ}$.

In an actual accelerometer, the quasi-steady component of error may vary slowly throughout a run, and will vary from run to run. It is assumed, in figure 5, that this quasi-steady error is constant throughout a run, and is termed a bias. The value of bias chosen is the maximum

anticipated steady-state error and, therefore, represents the worst possible case. Thus the curves for $U_{xp}$ shown in figure 5, together with their images reflected about the zero error line (which would represent runs with negative bias), represent an envelope of all possible errors for an accelerometer with an output uncertainty equal to the bias used.

For errors in the platform Z accelerometer, $U_{zp}$, the worst possible case is not represented by constant bias throughout the run because of the cancellation of error that occurs. However, until the range angle approaches $\pi/2$ (approximately 1200 sec. for all vehicles and conditions) constant bias does represent the worst case, and so the curves on figure 5 for $U_{zp}$ bias, plus their images, do represent an envelope of possible errors up to 1200 seconds. Thus comparisons of errors caused by $U_{zp}$ should be made at a time prior to this range angle. The time at which the range angle becomes $\pi/2$ is indicated on this and subsequent figures.

Figure 6 shows, for the standard vehicle and conditions, the effect on the altitude error of switching out the accelerometers for a while after $\tau_3$; $\tau_4$ is the time at which both the accelerometers were switched in again. Since $\tau_3 = 27$ seconds (for this value of $\Delta V$) the curve with $\tau_4 = 27$ seconds is actually one for which the accelerometers are not switched out at all. Figure 6(a) shows that the error due to $U_{xp}$ bias can be reduced by switching both accelerometers out, and the optimum switch-in time appears to be at about 700 seconds. From a comparison of this with the time histories in figures 2(a) and (c) and the altitude versus acceleration curves of figure 2(d), it can be seen that at 700 seconds, $f_\gamma$ is about half the bias level and $f_\alpha$ is approximately equal to the bias level, so that if the accelerometers were turned on when their output reached the bias level, the results would be nearly optimum.

Figure 6(b) shows the same thing for errors caused by $U_{zp}$. Again the optimum switch-in time appears to be about 700 seconds.

Figure 7 shows the effect of turning off only one accelerometer when both $U_{xp}$ and $U_{zp}$ errors are present, in comparison with curves where neither or both accelerometers are switched out. This comparison is valid only out to about 1200 seconds because of the change in sign of the error due to $U_{zp}$. However, one can see that with both accelerometers switched out until $t = 710$ seconds the error at this point is smaller than one would get if either were switched out by itself. The case with both accelerometers in all the time appears to give smaller errors than with just $f_{zm}$ out. However, this is misleading, since, for the particular values of bias chosen, there is a cancellation of the errors from $U_{zp}$ and $U_{xp}$. If one of the biases were negative, the errors would add, and the case with both accelerometers in would then give larger errors than the case with $f_{zm}$ out.

Figure 8 shows the effect of switching out the accelerometers, and turning them on again individually when their resolved outputs ($f_\alpha$ and $f_\gamma$)

are twice the bias level. This is shown for a variety of conditions and, for each condition, is compared with the corresponding results when the accelerometers are not switched out at all. It can be seen that switching the accelerometers out leads to reduced errors for all conditions.

The time at which the range angle becomes $\pi/2$ is shown on each figure, and the errors from $U_{zp}$, beyond this point no longer represent the worst possible cases.

Altitude errors at the end of the run (h = 100,000 ft), caused by various error producing sources acting singly, are summarized in table I for the standard vehicle starting from $h_o$ = 677,000 feet with $\Delta V$ = 250 feet per second. Also shown in the table are altitude rate error, range error, and range rate error. The errors caused by the accelerometer biases are shown with the accelerometers switched in all the time, and also switched out for the optimum time. Finally, the effect of all errors, simultaneously applied, for both conditions, is shown. Here, the errors are combined on an RMS basis, since one would not expect maximum errors from all sources simultaneously.



## CONCLUDING REMARKS

From these data, it can be determined that an inertial navigation system can provide a re-entry vehicle with the required position and velocity information during the re-entry, in spite of the instability of the system equations. There will be errors but even for only fair inertial navigation equipment, with fairly good initial information, these errors do not become excessive.

The errors from any source build up with time, so that those re-entries which take the least time will produce the smallest errors. The sooner radio contact is re-established with the ground the smaller the errors will be.

Further, although switching out the accelerometers does reduce the error from accelerometer bias, the errors caused by other sources are as large as those caused by the accelerometers. Thus the complexity of switching out the accelerometers may not be warranted.

Ames Research Center
National Aeronautics and Space Administration
Moffett Field, Calif., March 21, 1960

# APPENDIX A

## DERIVATION OF ALTITUDE INSTABILITY

The first of equations (5) and (10) can be used to show the altitude instability mentioned in the introduction. Since $h \ll R_r$, the gravity term in each equation may be linearized, by means of the binomial expansion, as follows:

$$\frac{g_r R_r^2}{(R_r + h)^2} = \frac{g_r}{\left(1 + \frac{h}{R_r}\right)^2} = g_r \left(1 - \frac{2h}{R_r} + \cdots\right) \tag{A1}$$



Substituting this into equation (5) and a similar expression in $h_i$ into (10), and collecting terms in $h$ or $h_i$ gives:

$$\left.\begin{aligned} \ddot{h} - h\left(\dot{\theta}^2 + 2\frac{g_r}{R_r}\right) &= R_r\dot{\theta}^2 - g_r - f_\gamma \\ \ddot{h}_i - h_i\left(\dot{\theta}_i^2 + 2\frac{g_r}{R_r}\right) &= R_r\dot{\theta}_i^2 - g_r - f_{zm} \end{aligned}\right\} \tag{A2}$$

When the vehicle speed is considerably less than orbital, so that $\dot{\theta}^2 \ll g_r/R_r$,[1] these equations become:

$$\left.\begin{aligned} \ddot{h} - \frac{2g_r}{R_r} h &= -g_r - f_\gamma \\ \ddot{h}_i - \frac{2g_r}{R_r} h_i &= -g_r - f_{zm} \end{aligned}\right\} \tag{A3}$$

The equation for altitude error can be obtained by subtracting these two equations:

$$(\ddot{h}_i - \ddot{h}) - \frac{2g_r}{R_r}(h_i - h) = -(f_{zm} - f_\gamma) \tag{A4}$$

or

$$\ddot{h}_\epsilon - \frac{2g_r}{R_r} h_\epsilon = -(f_{zm} - f_\gamma) \tag{A5}$$

---

[1] At orbital speed $\dot{\theta}^2 = g_r/R_r$

When solved, this equation has an unstable root of the form $Ke^{t/\sqrt{R_r/2g_r}}$ with $\sqrt{R_r/2g_r}$ about 10 minutes. This period does not change appreciably until the vehicle velocity becomes about 0.8 of orbital velocity.

This unstable solution for altitude error will have a magnitude K which is proportional to any initial altitude error, and to any subsequent error in measuring acceleration. Thus one possibility for reducing the error caused by this instability is to reduce the accelerometer measurement error. In particular, if the anticipated measurement error is larger than the magnitude of the true acceleration, it would seem that zero would be the best value of acceleration to use in computing $h_i$.

## REFERENCES

1. Synge, J. L., and Griffith, B. A.: Principles of Mechanics. McGraw-Hill Book Co., Inc., 1942.

2. Anon.: Abbreviated English Tables of the ARDC Model Atmosphere 1956. Geophysic Research Directorate, Air Force Cambridge Research Center, ARDC.

3. Breakwell, J. V., and Koehler, L. F.: Elliptical Orbit Lifetimes. American Astronautical Society, Preprint No. 58-34, 1958.

TABLE I.- ALTITUDE ERROR AT END OF ENTRY FOR A STANDARD VEHICLE ENTERING FROM 677,000 FEET WITH A $\Delta V$ OF 250 FEET PER SECOND

| Error source and magnitude | Error at 100,000 feet | | | |
|---|---|---|---|---|
| | $h_\epsilon$, ft | $\theta_\epsilon$, radian | $\dot{h}_\epsilon$, ft/sec | $\dot{\theta}_\epsilon \times 10^6$, radian/sec |
| $h_{\epsilon o}$ = 500 ft | 5,427 | -0.0002 | 10.1 | -0.094 |
| $\theta_{\epsilon o}$ = $10^{-4}$ radian | -811 | .0001 | -2.9 | -.0292 |
| $\dot{h}_{\epsilon o}$ = 1 ft/sec | 1,598 | -.0001 | 3.6 | -.00052 |
| $\dot{\theta}_{\epsilon o}$ = $5(10)^{-8}$ radian/sec | 5,121 | -.0002 | 8.9 | .1165 |
| $\omega_d$ = $2(10)^{-7}$ radian/sec | -2,902 | -.0000 | -10.8 | .1207 |
| Accelerometer bias = $10^{-4}g$ | | | | |
| $U_{xp}$ Accelerometers in all the time[1] | 13,192 | -.0004 | 23.9 | .389 |
| $U_{zp}$ Accelerometers in all the time[1] | -883 | .0001 | .9 | .218 |
| $U_{xp}$ Accelerometers out for optimum time[1] | 6,583 | -.0002 | 12.2 | .238 |
| $U_{zp}$ Accelerometers out for optimum time[1] | 112 | .0001 | 1.3 | .098 |
| RMS sum[2] Accelerometers in all the time | 15,400 | .0005 | 29.7 | .487 |
| RMS sum[2] Accelerometers out for optimum time | 10,400 | .0004 | 21.4 | .324 |

[1]The errors caused by $U_{zp}$ are given for a time of 1260 seconds (where $\theta = \pi/2$).

[2]In computing the RMS sum, it was assumed that the errors caused by $U_{zp}$ remained constant subsequent to 1260 seconds. The actual error from the worst case was not determined and could be larger than the assumed error.

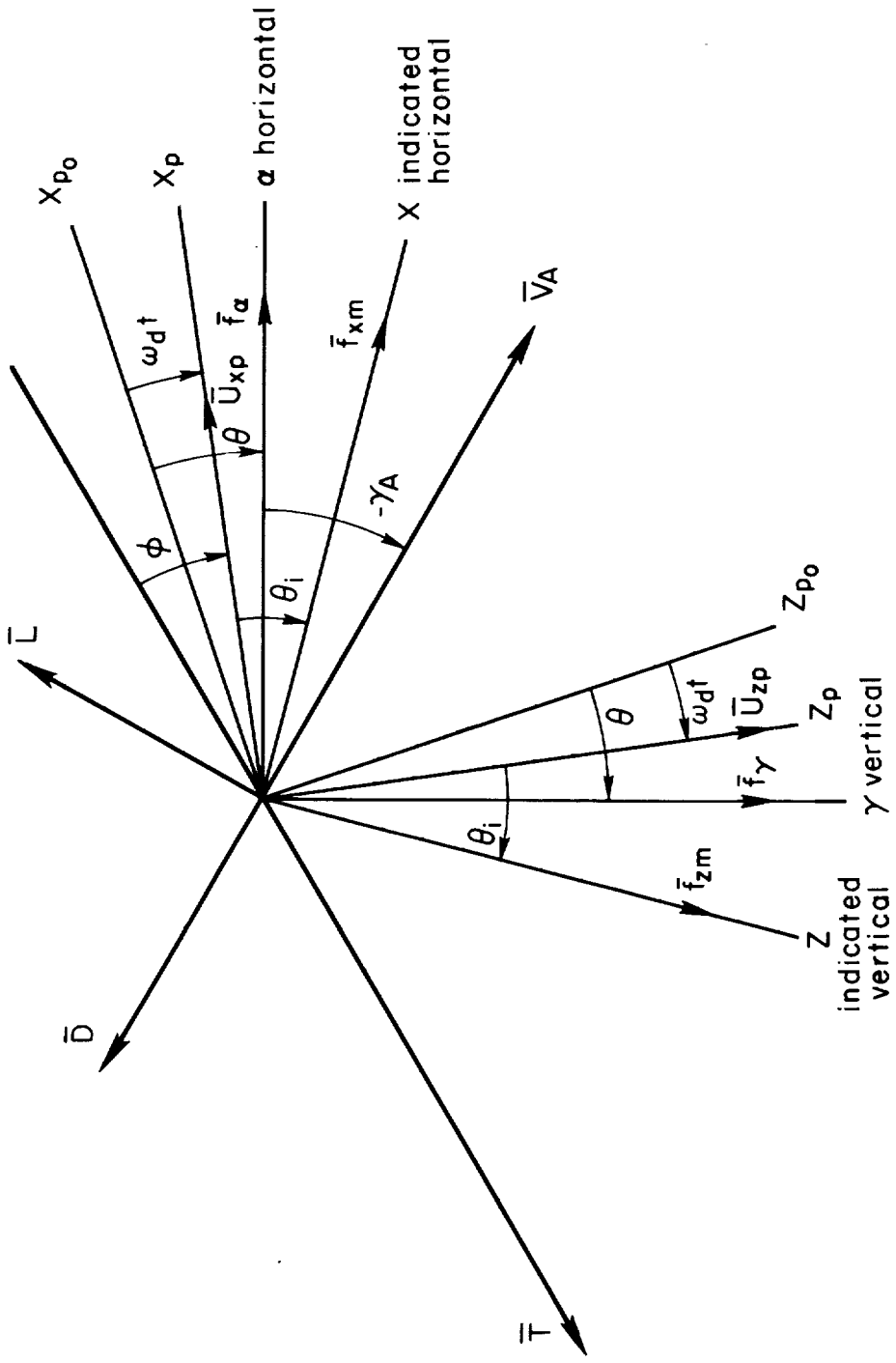


(a) Vehicle centered.

Figure 1.- Coordinates and vectors.

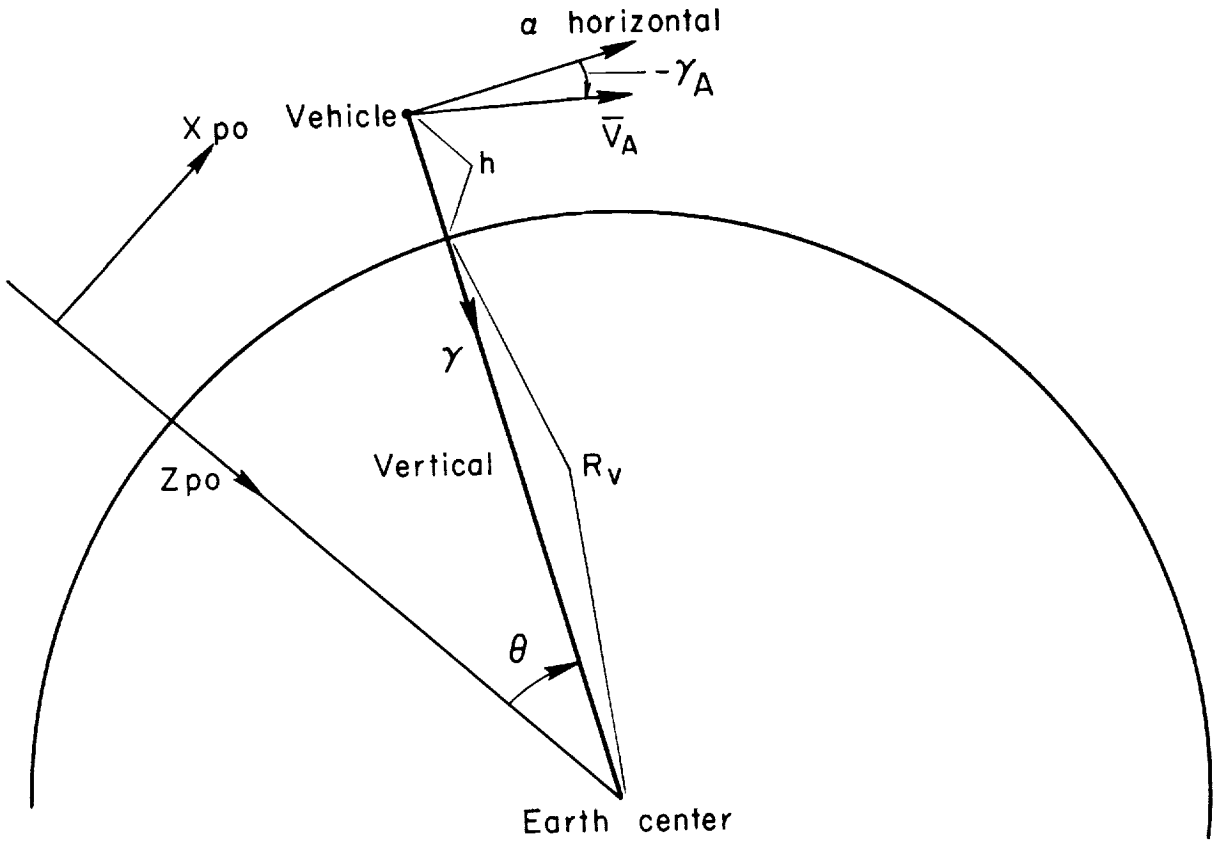


(b) Earth centered.

Figure 1.- Concluded.

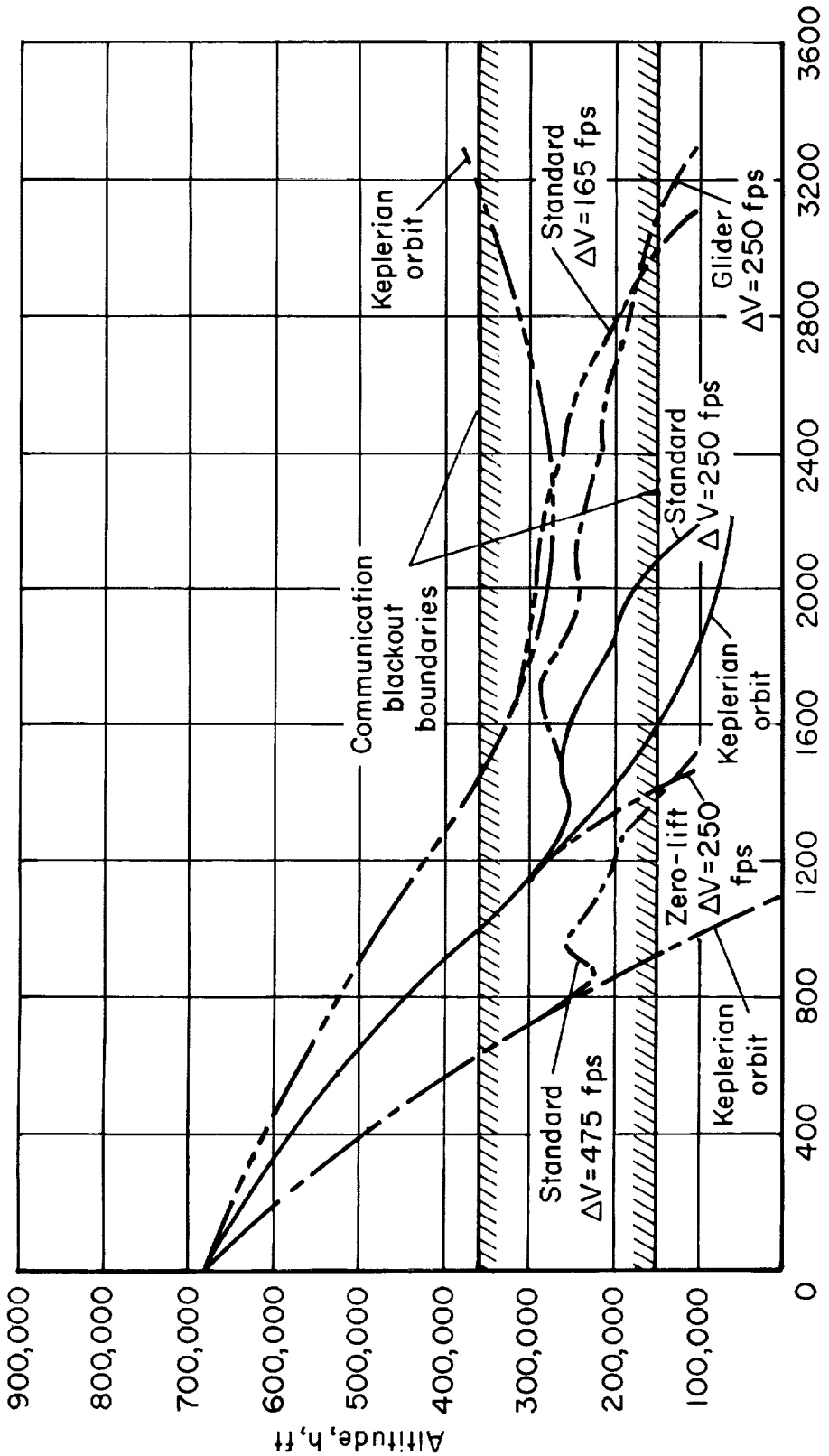


(a) Altitude versus time for 677,000 feet initial altitude.

Figure 2.- Flight-path profile for different conditions and vehicles.

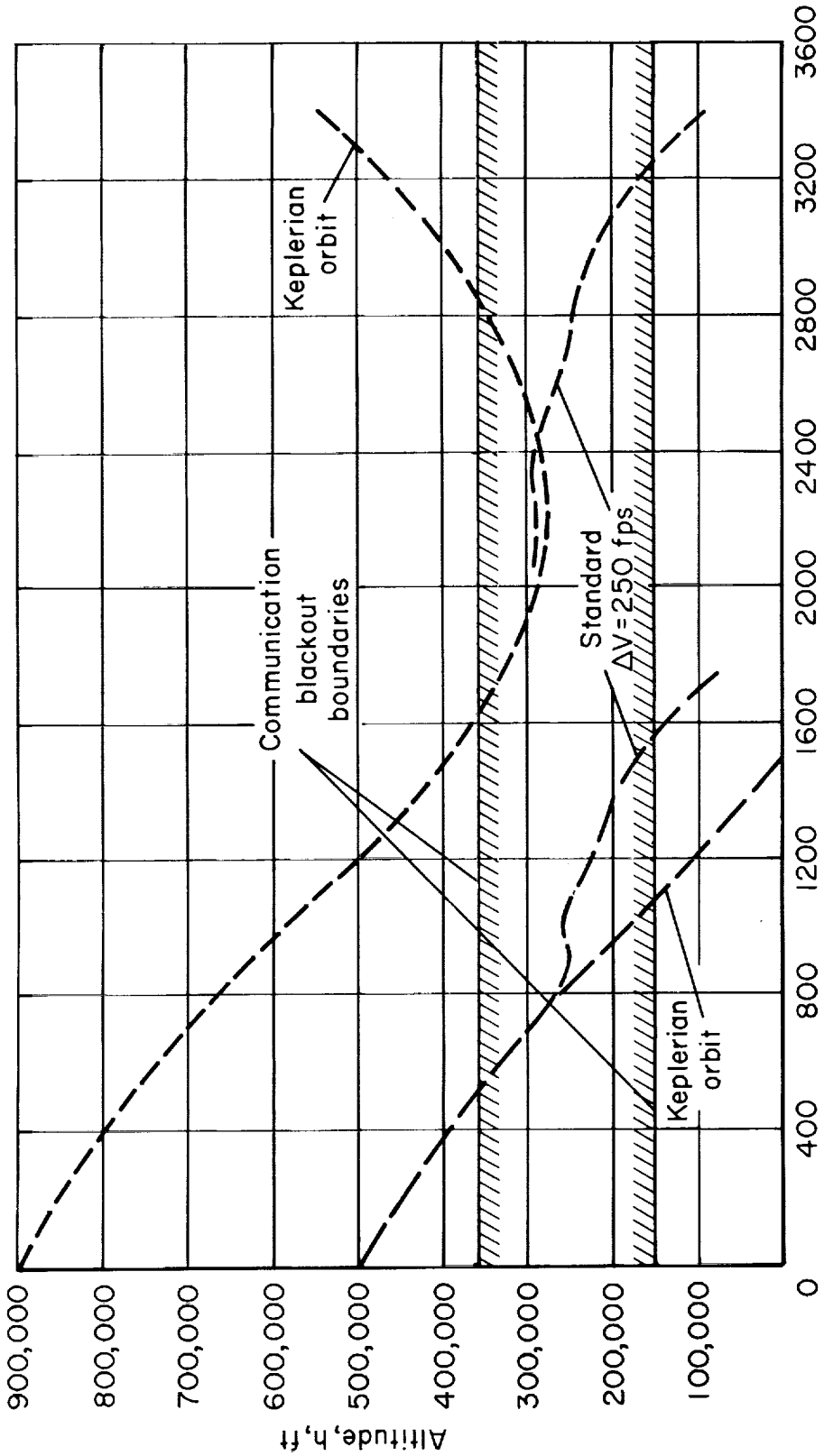


(b) Altitude versus time for other initial altitudes.

Figure 2.- Continued.

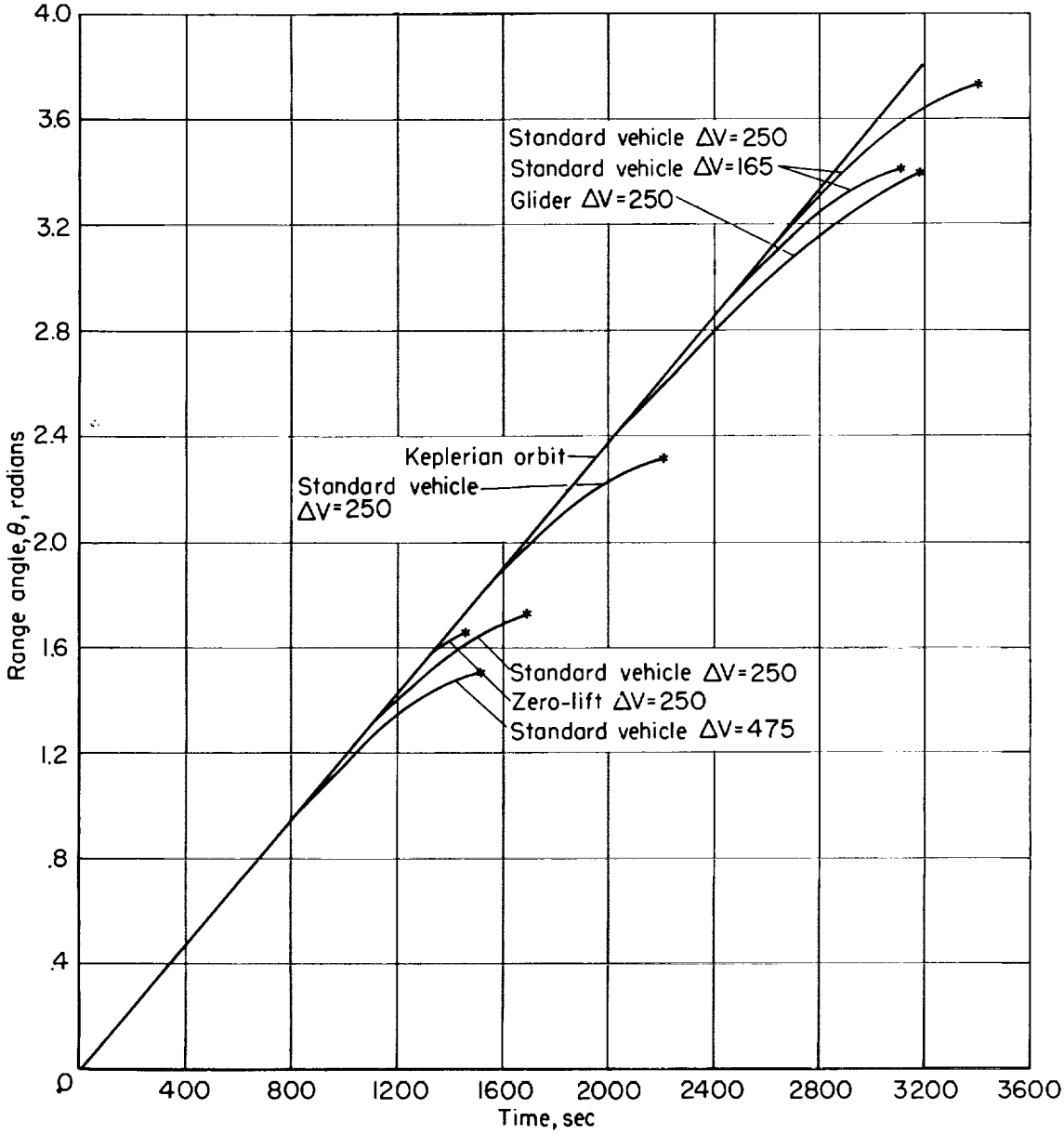


(c) Range versus time.

Figure 2.- Continued.

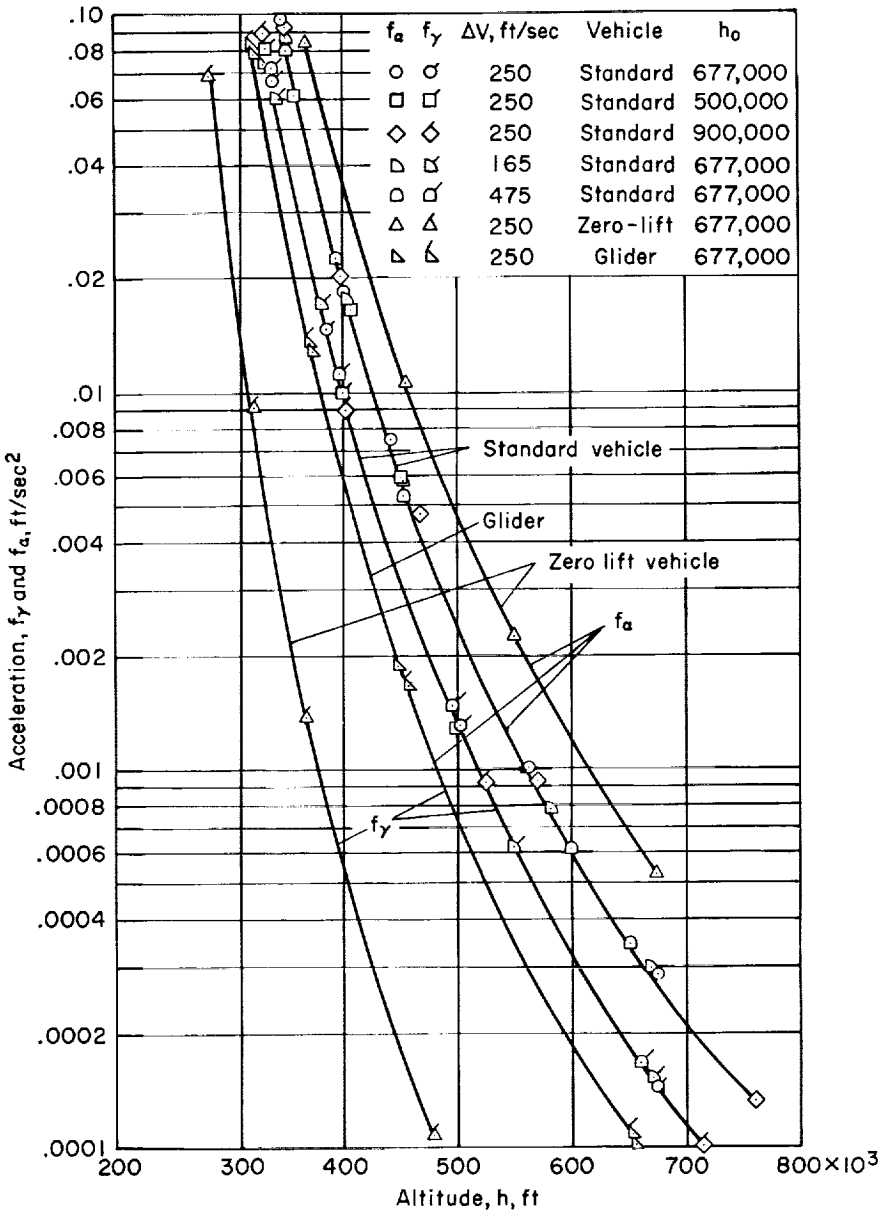


(d) Acceleration versus altitude.

Figure 2.- Concluded.

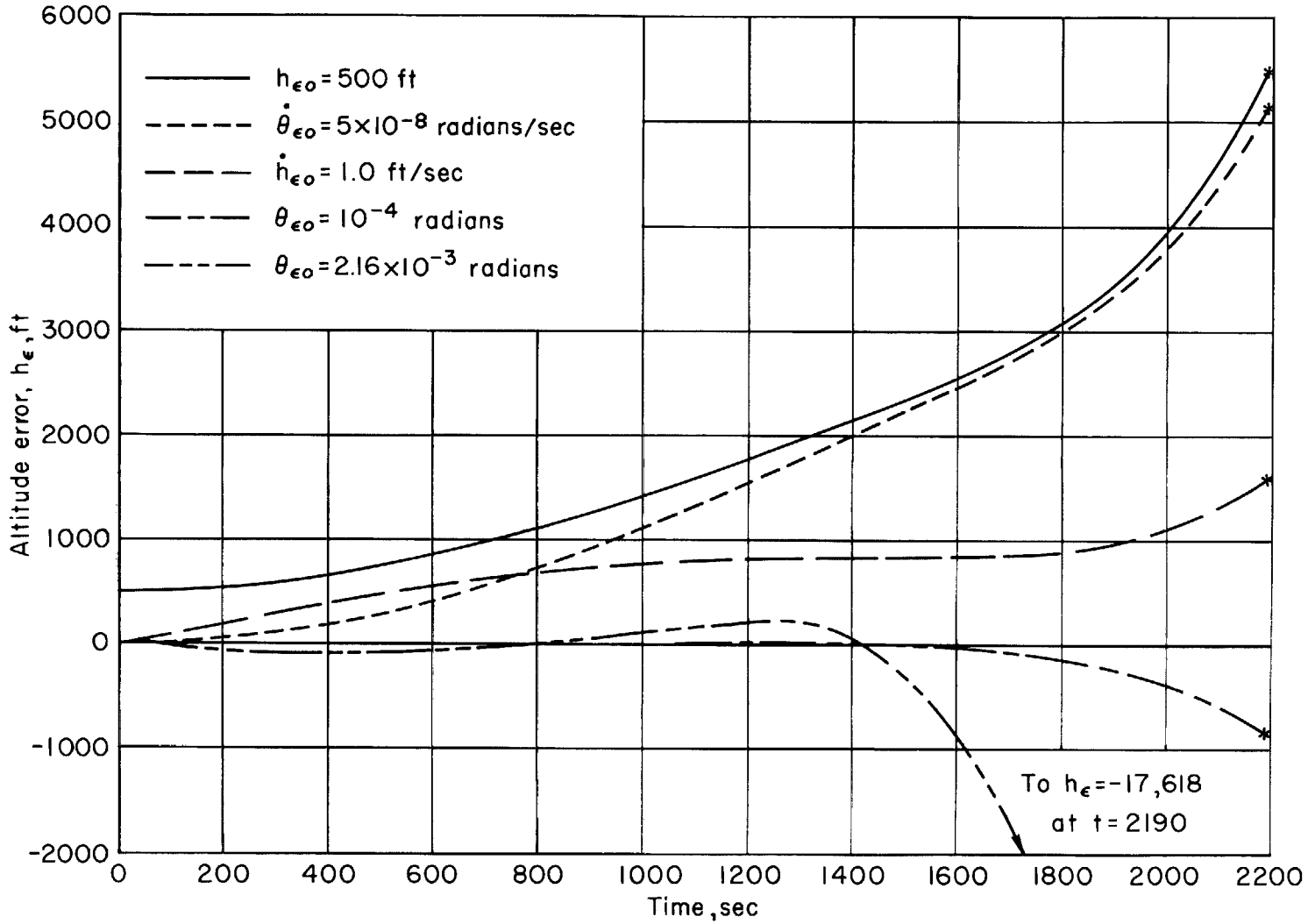


(a) Standard vehicle and basic conditions.

Figure 3.- Altitude error resulting from various initial condition errors.

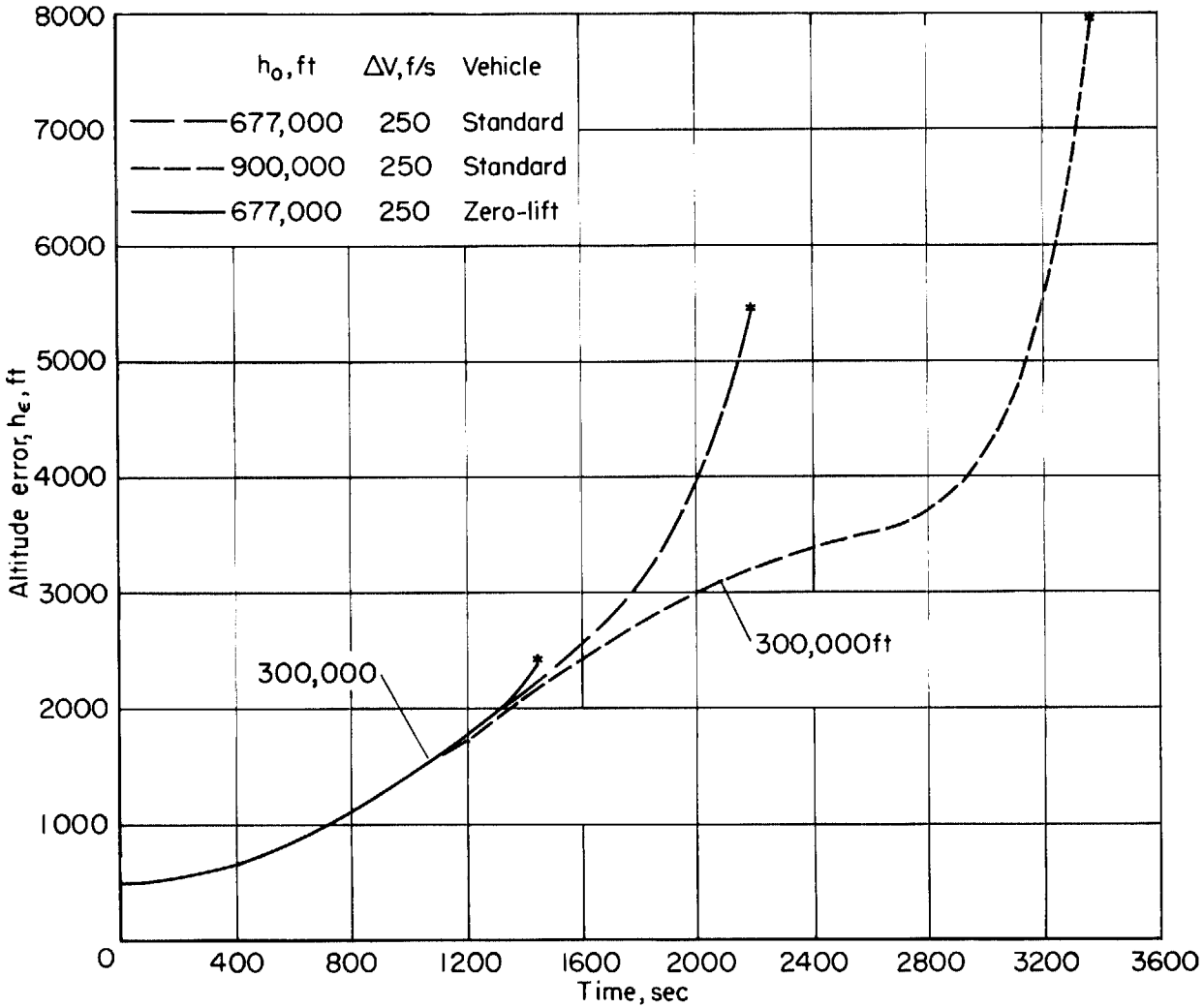


(b) Various vehicles and conditions.

Figure 3.- Concluded.

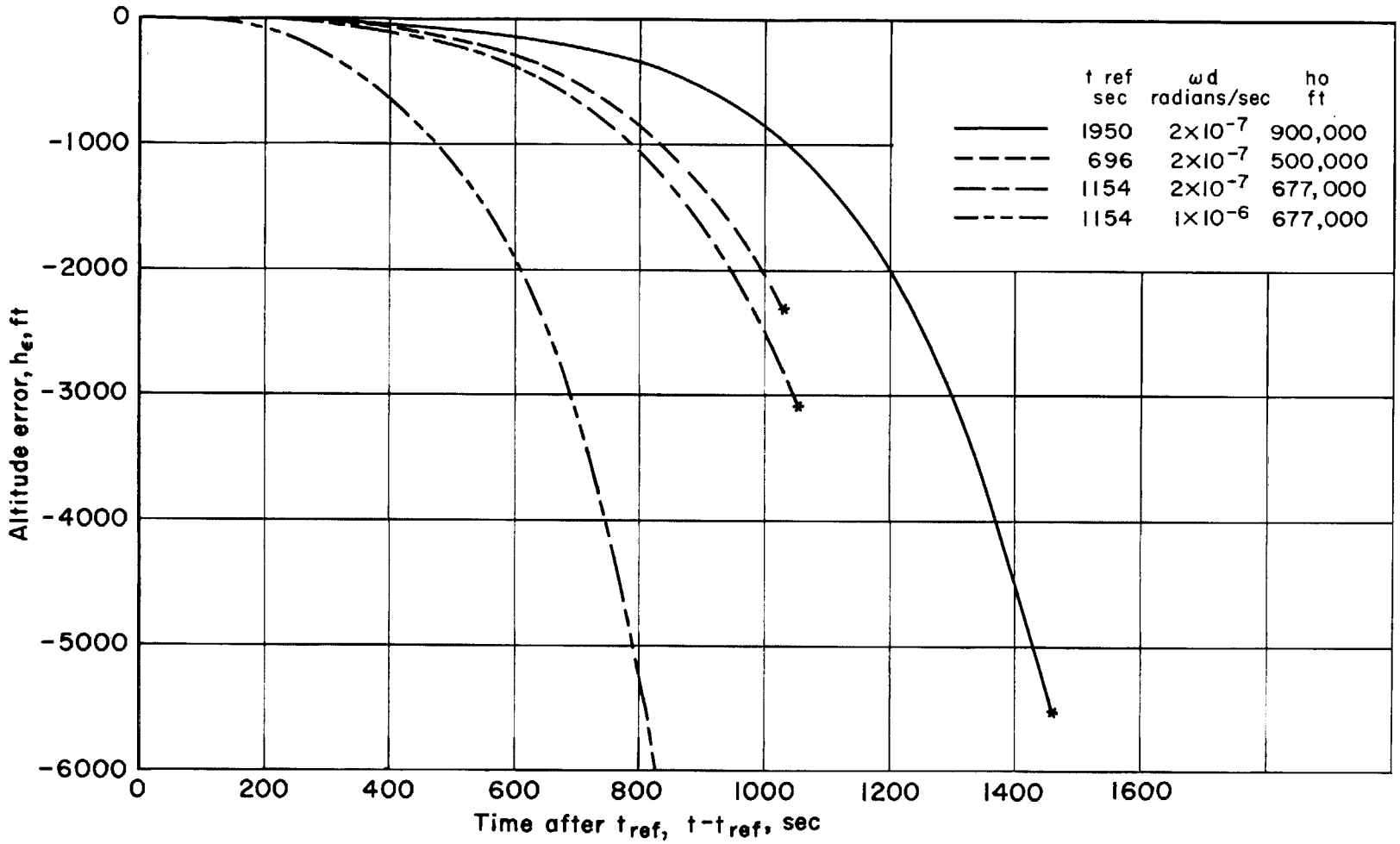


Figure 4.- Effect of gyro drift on altitude errors for standard vehicle.

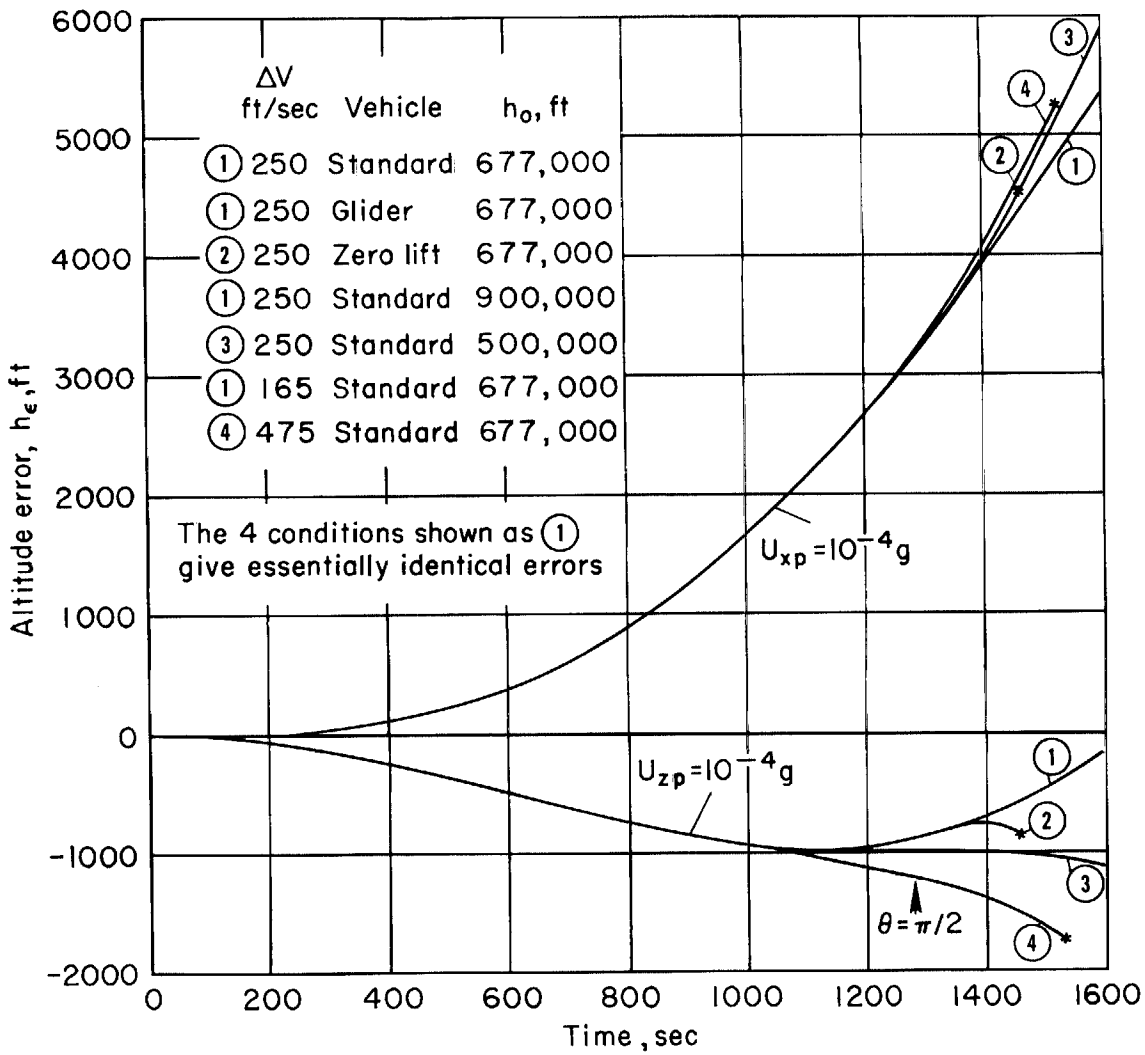


Figure 5.- Altitude errors from accelerometer biases for different conditions and vehicles.

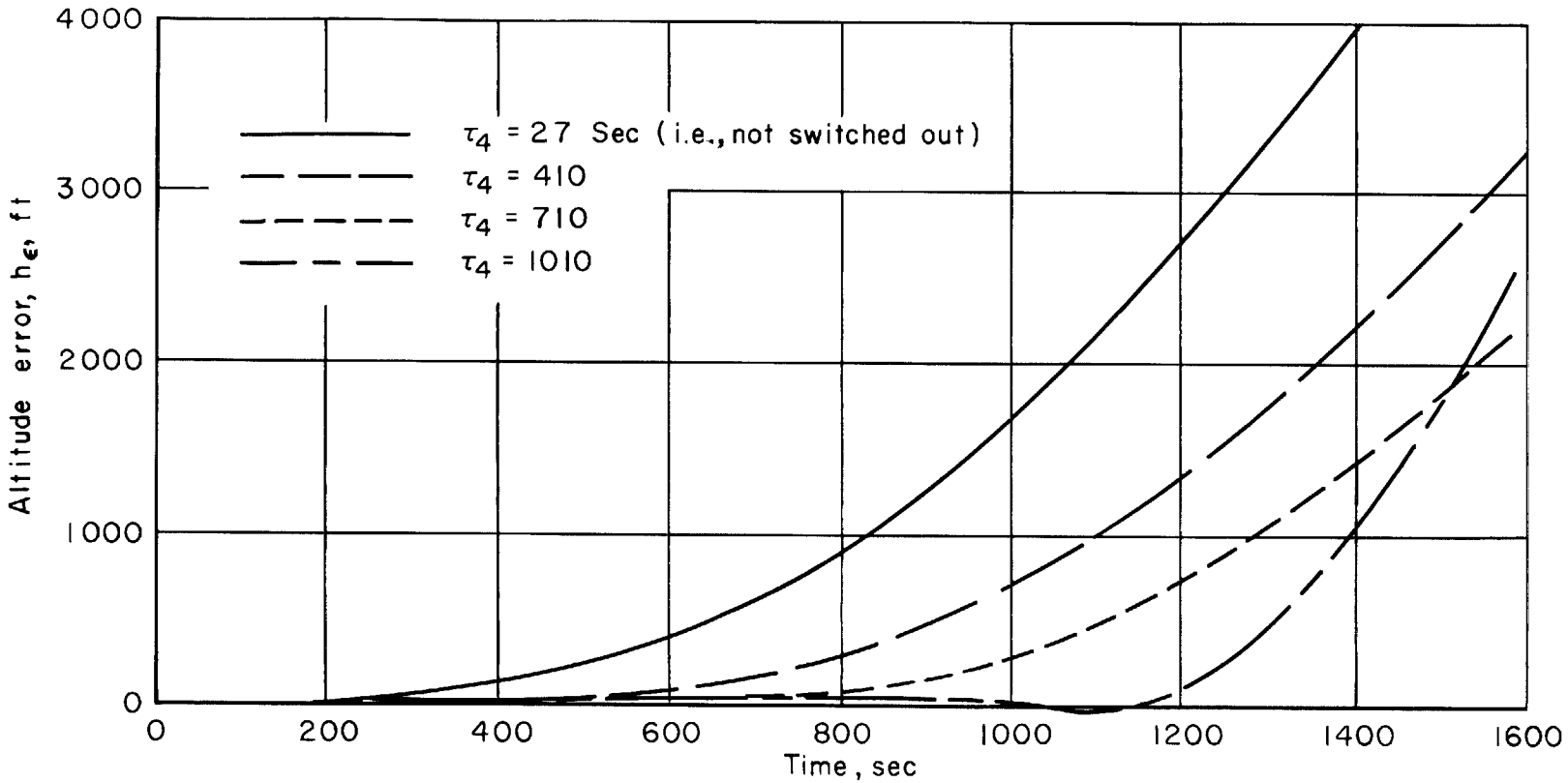


(a) Error caused by $U_{xp}$.

Figure 6.- Effect of accelerometer switch in time on altitude error for standard vehicle with basic conditions.

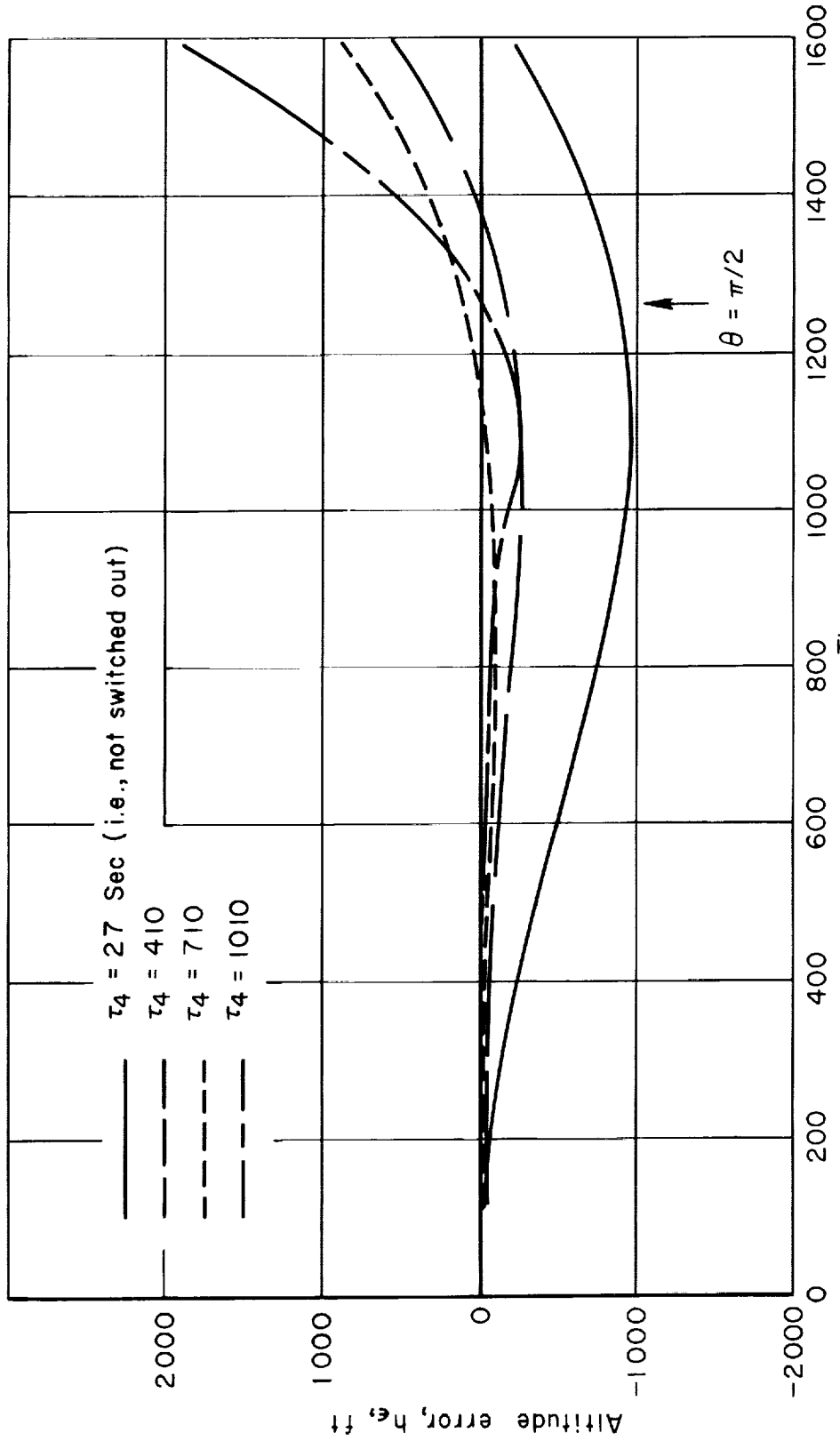


(b) Error caused by $U_{zp}$.

Figure 6.- Concluded.

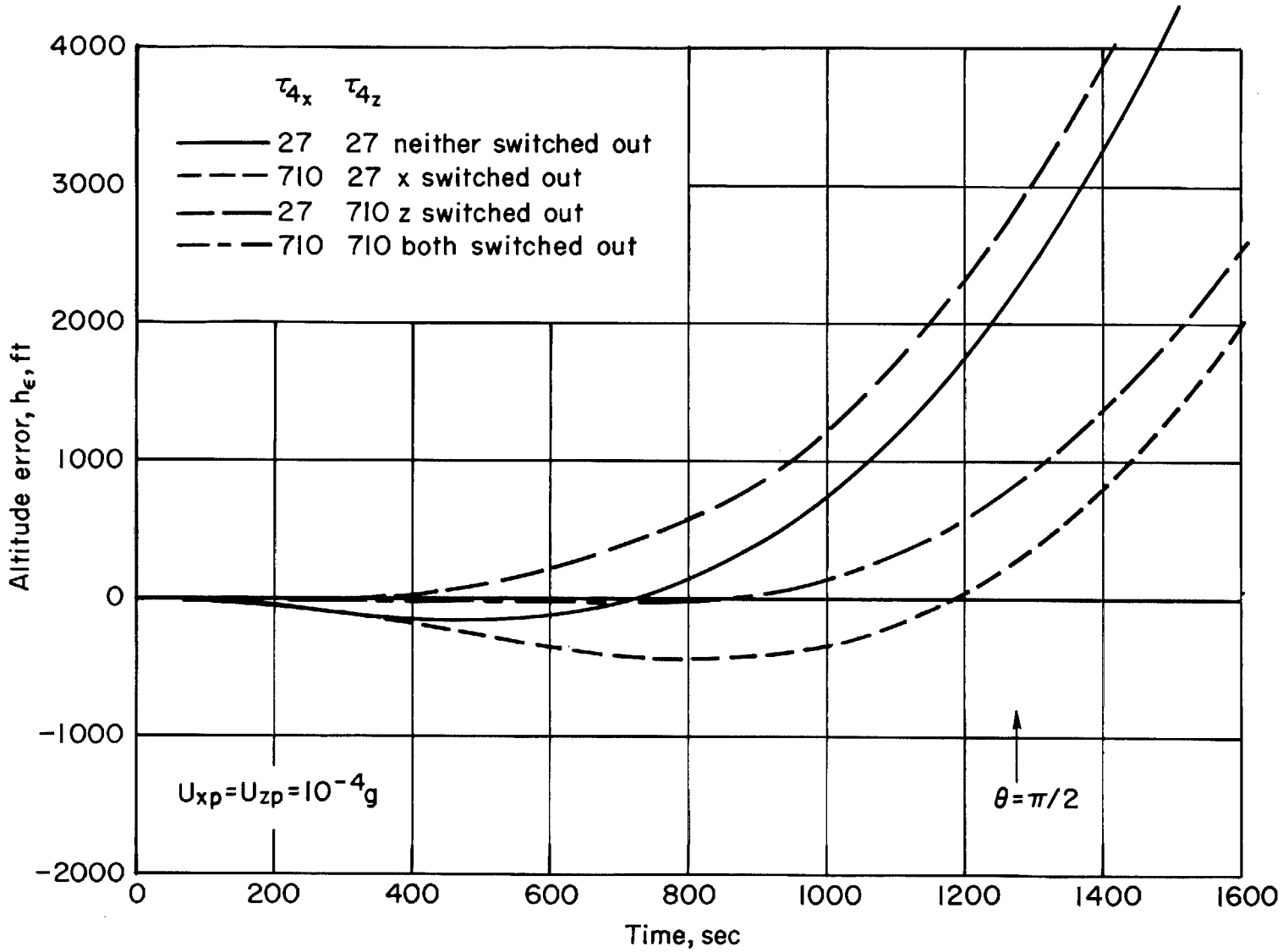


Figure 7.- Effect of switching out one or both accelerometers on altitude error for standard vehicle with basic conditions.

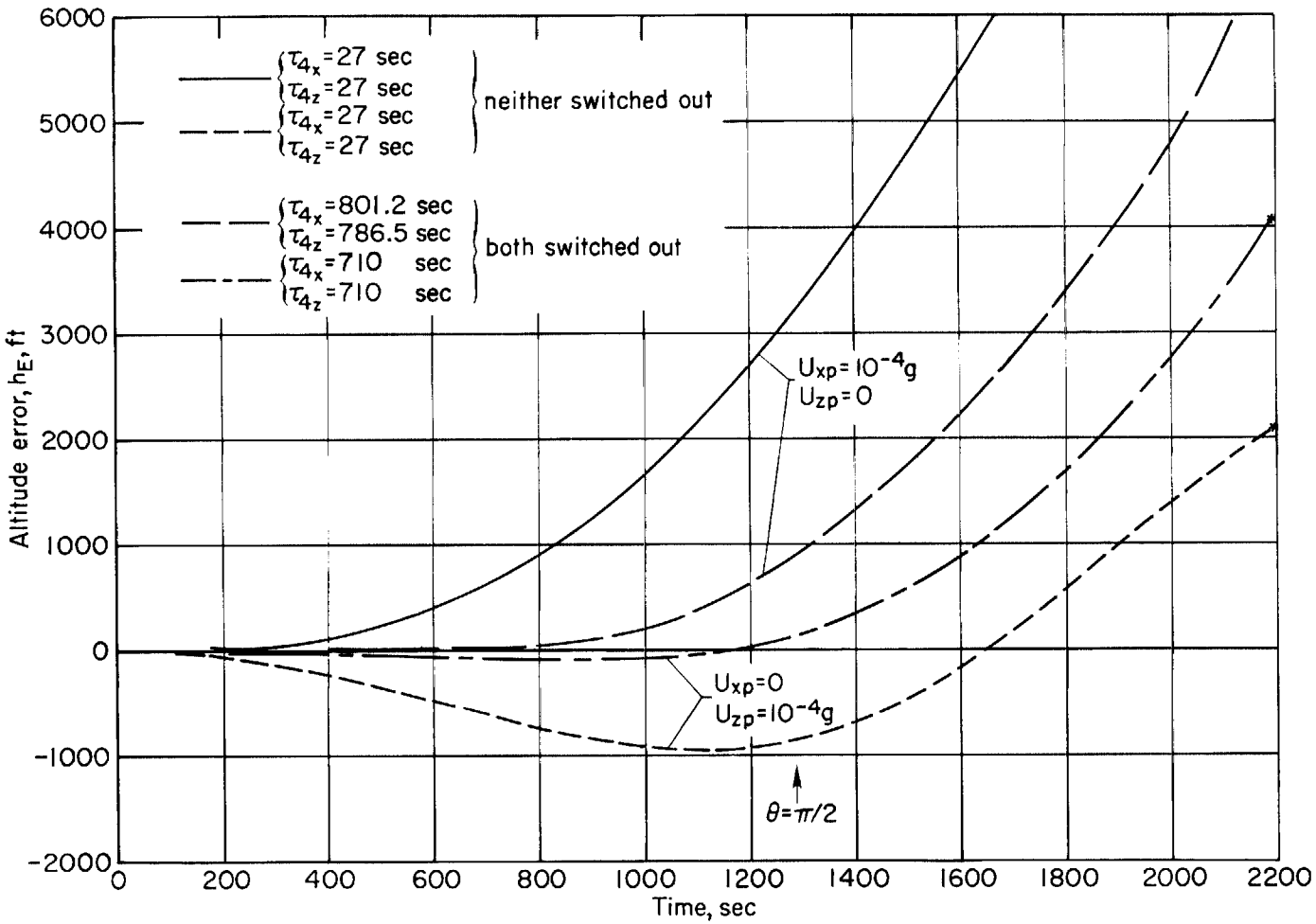


(a) Standard vehicle with basic conditions.

Figure 8.- Effect of turning off accelerometers for various conditions.

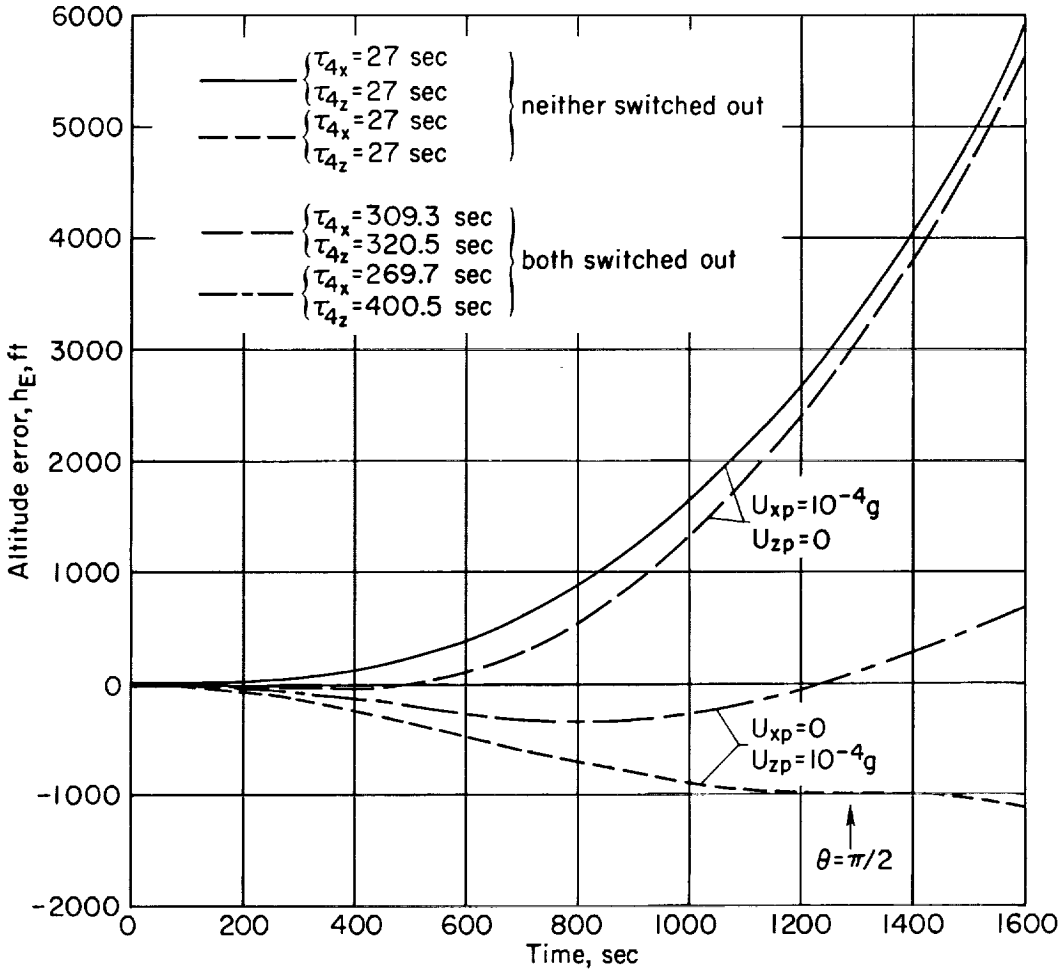


(b) 500,000 feet altitude, standard vehicle and $\Delta V$ = 250 feet per second.

Figure 8.- Continued.

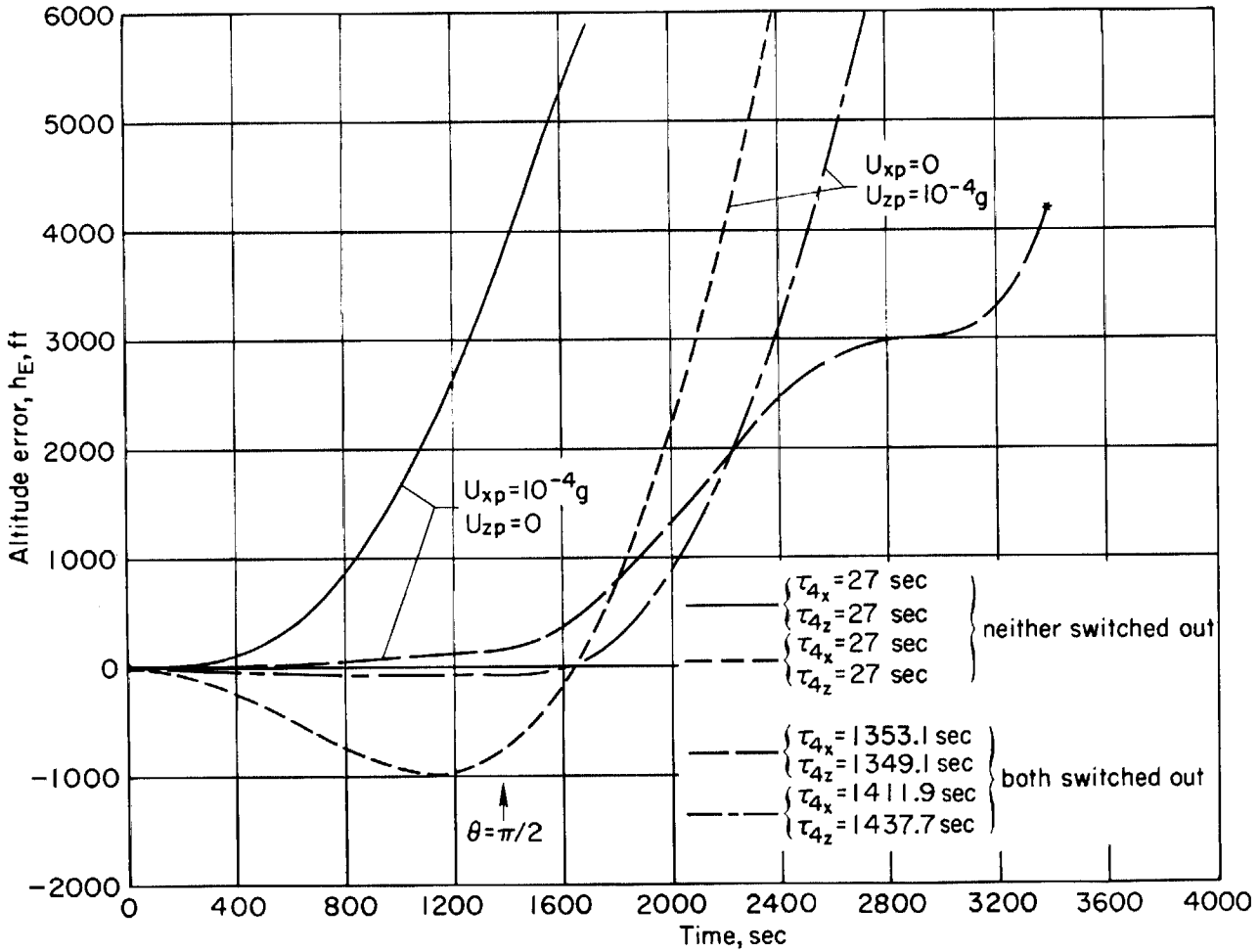


(c) 900,000 feet altitude, standard vehicle and $\Delta V$ = 250 feet per second.

Figure 8.- Continued.

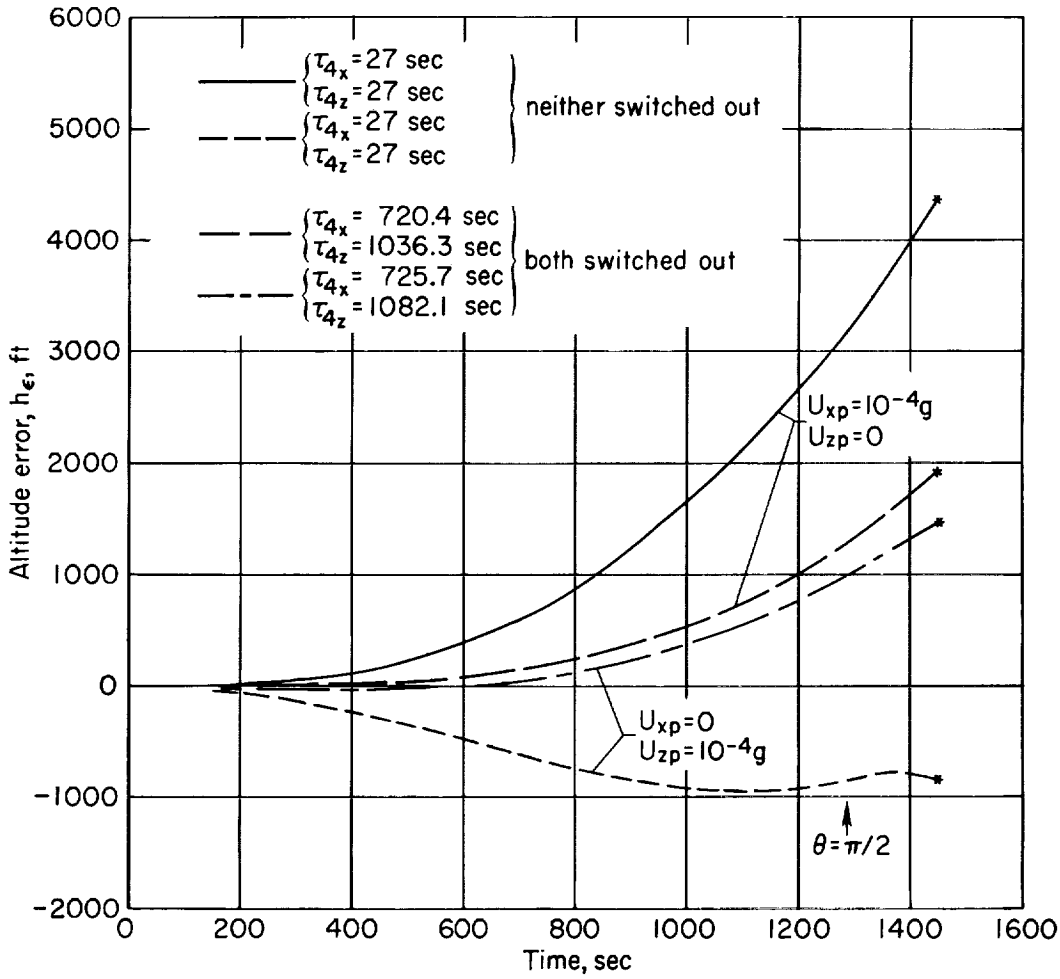


(d) Zero-lift vehicle, basic conditions.

Figure 8.- Continued.

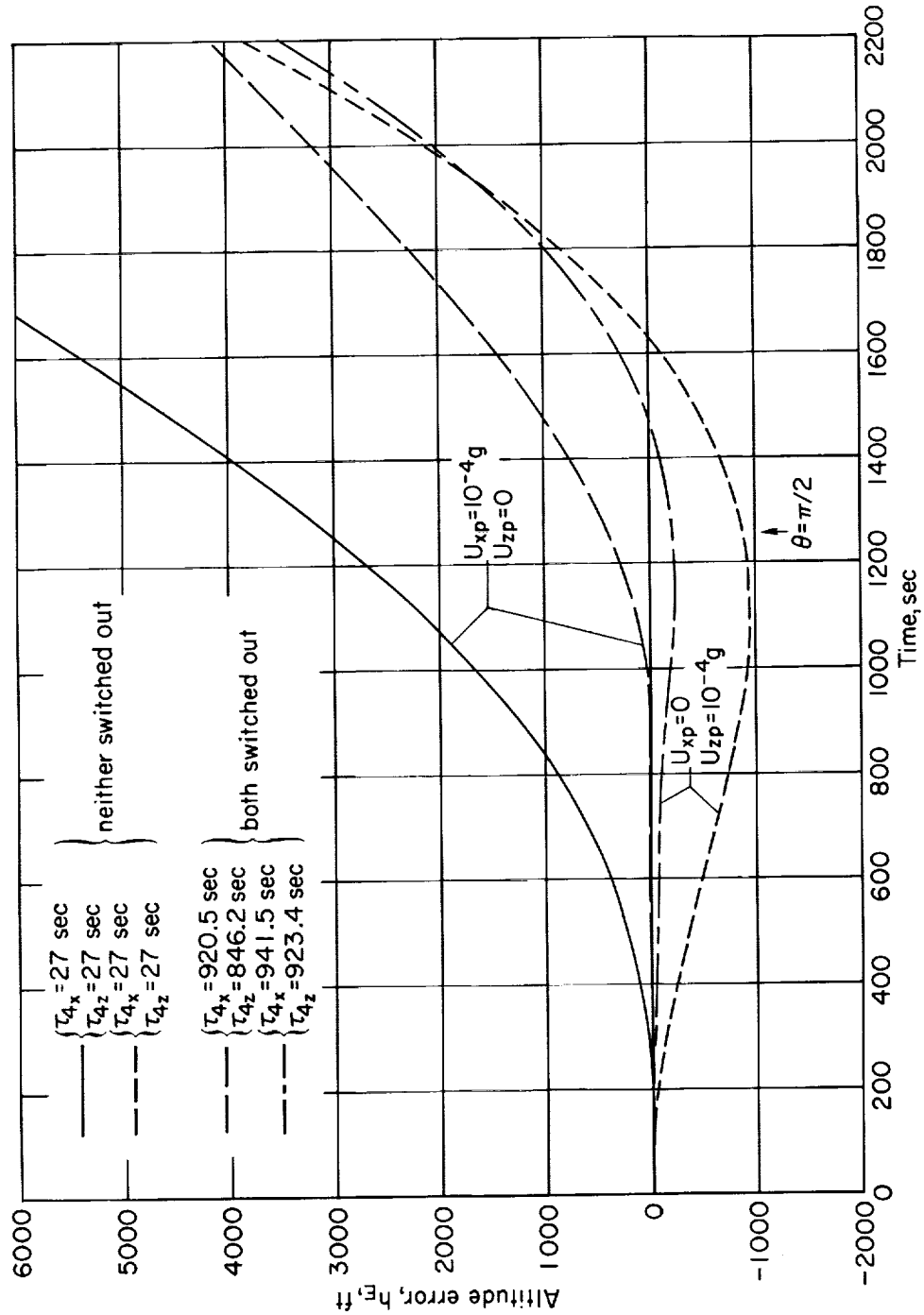


(e) Glider vehicle, basic conditions.

Figure 8.- Continued.

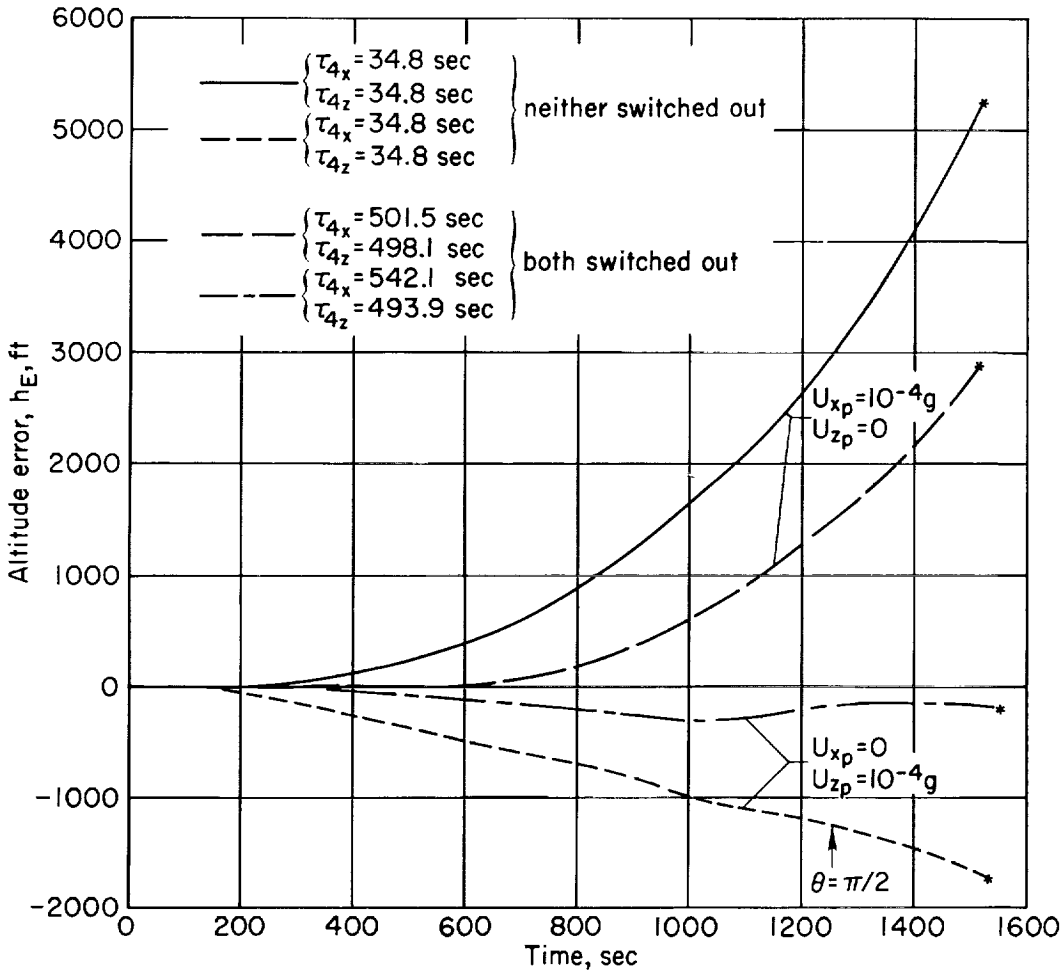


(f) Standard vehicle, $h_o$ = 677,000 feet, $\Delta V$ = 475 feet per second.

Figure 8.- Continued.

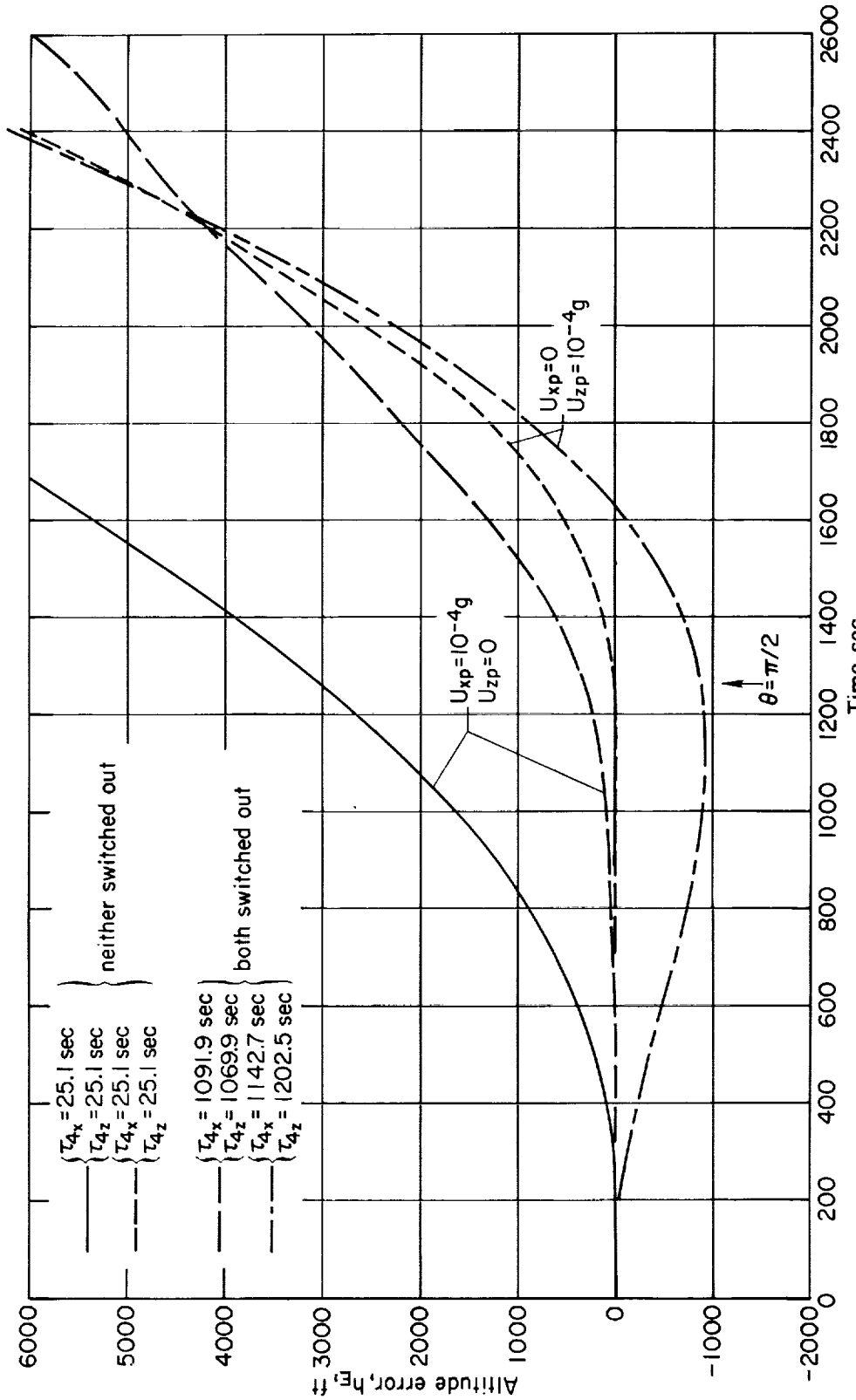


(g) Standard vehicle, $h_o$ = 677,000 feet, $\Delta V$ = 165 feet per second.

Figure 8.- Concluded.